ELECTRONIC SUPPORTING INFORMATION (ESI) to:

In vivo photoacoustic tumor tomography using a quinoline-annulated porphyrin as NIR molecular contrast agent

Michael Luciano,[a,#] Mohsen Erfanzadeh,[b,#] Feifei Zhou,[b] Zhu Hua,[a] Tobias Bornhütter,[c] Beate Röder,[c] Quing Zhu,[b,c,*] Christian Brückner[a,*]

Department of Chemistry, University of Connecticut, Storrs, CT 06269-3060, USA

Department of Biomedical Engineering, University of Connecticut, Storrs, CT 06269-4157, USA

Institut für Physik, Humboldt-Universität zu Berlin, Newtonstraße 15, 12489 Berlin, Germany

a Department of Chemistry, University of Connecticut

b Department of Biomedical Engineering, University of Connecticut

c Humboldt University

& Current address: Department of Biomedical Engineering, Washington University in St. Louis, St. Louis, MI 63105, USA

# Equal contributions

* Authors to whom correspondence should be addressed: e-mail: quing.zhou@uconn.edu (QZ), c.bruckner@uconn.edu (CB)

Table of Contents

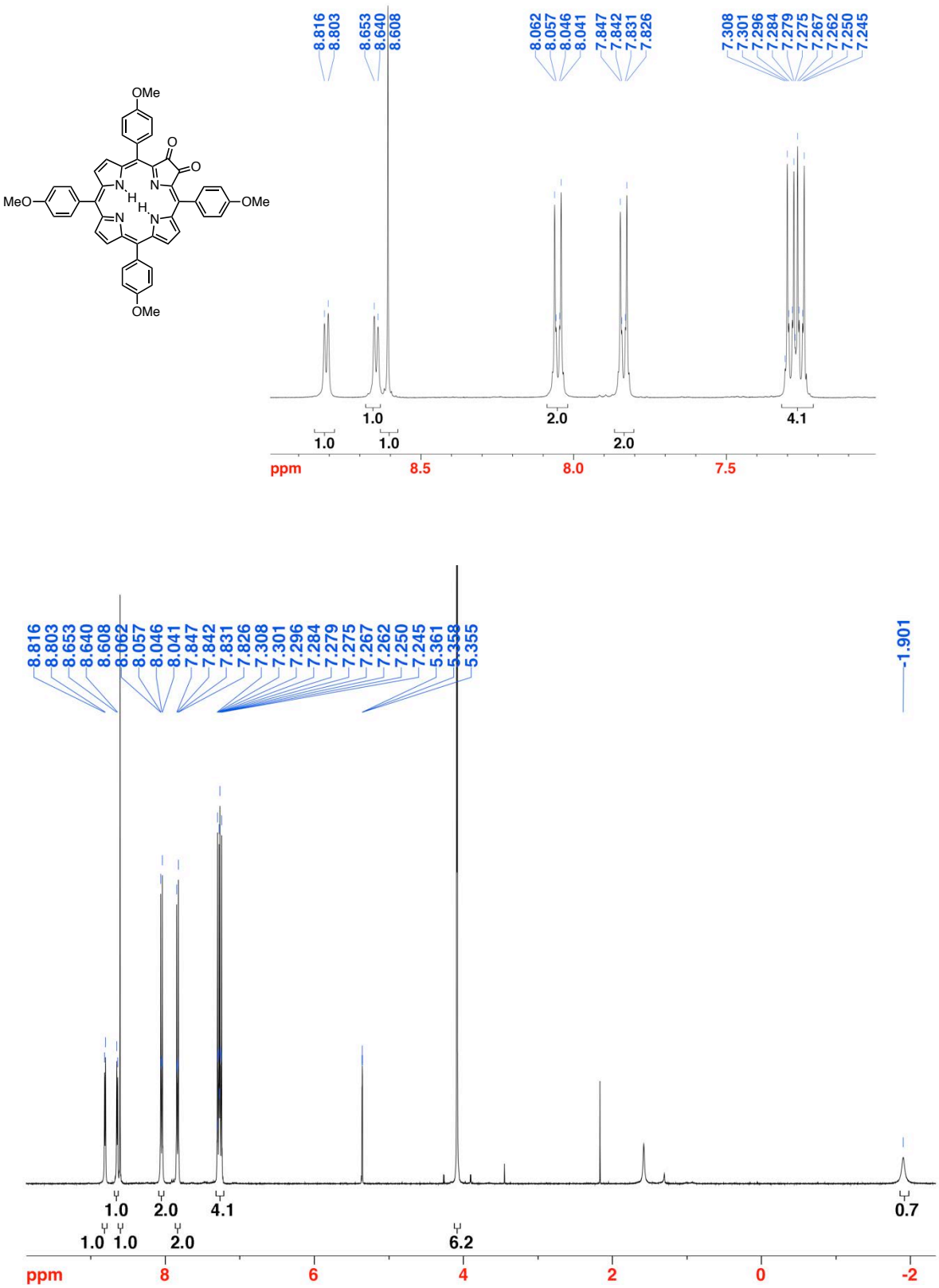

Figure S1. ^{1}H NMR spectrum (400 MHz, CD_2Cl_2) of **8**.

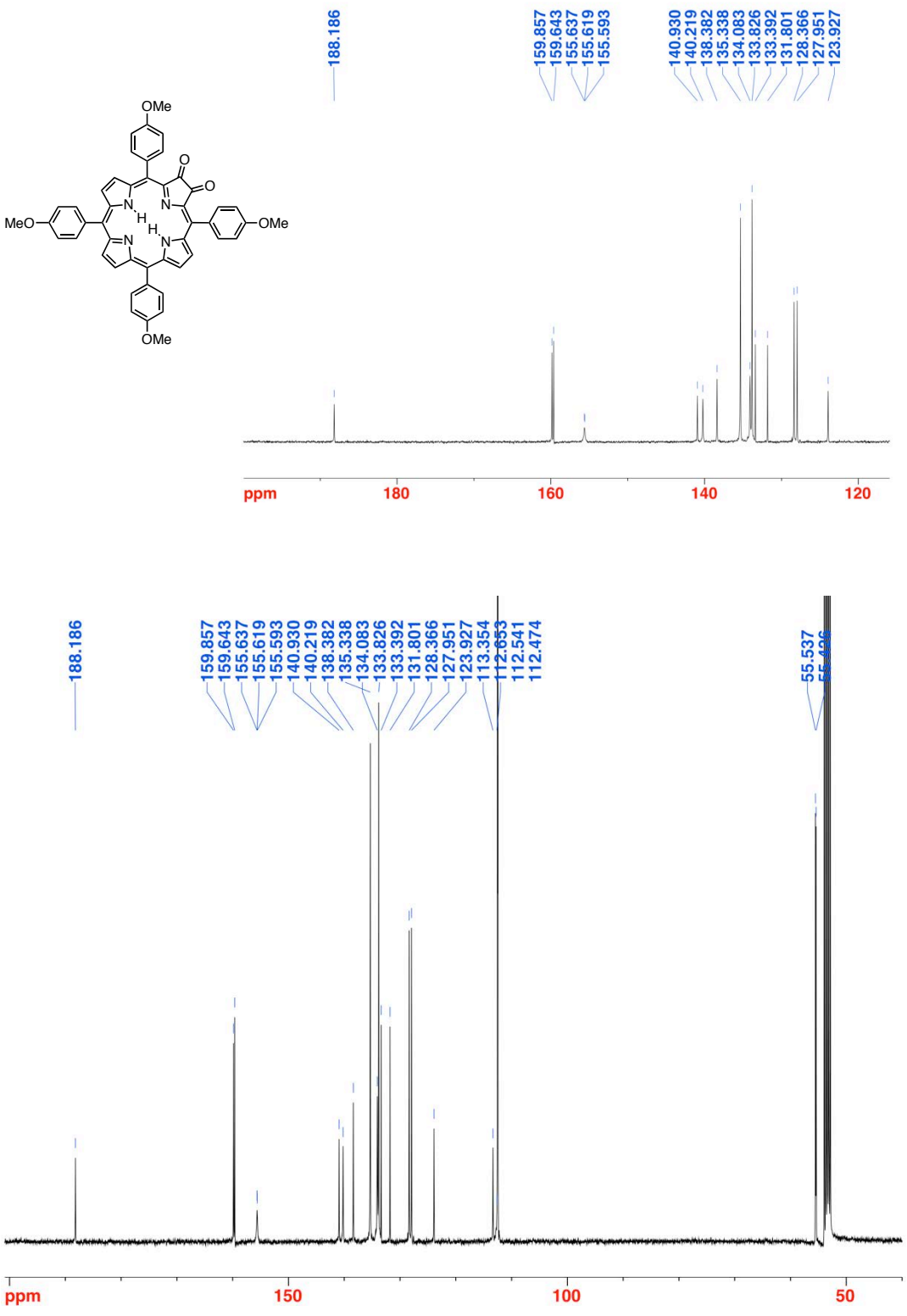

Figure S2. ^{13}C NMR spectrum (100 MHz, CD_2Cl_2) of **8**.

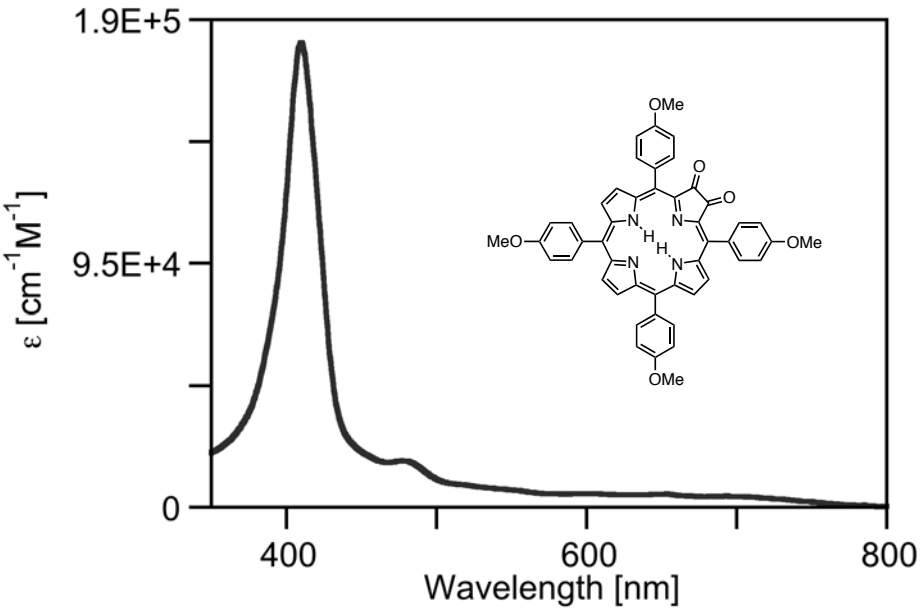

Figure S3. UV-vis spectrum (CH_2Cl_2) of **8**.

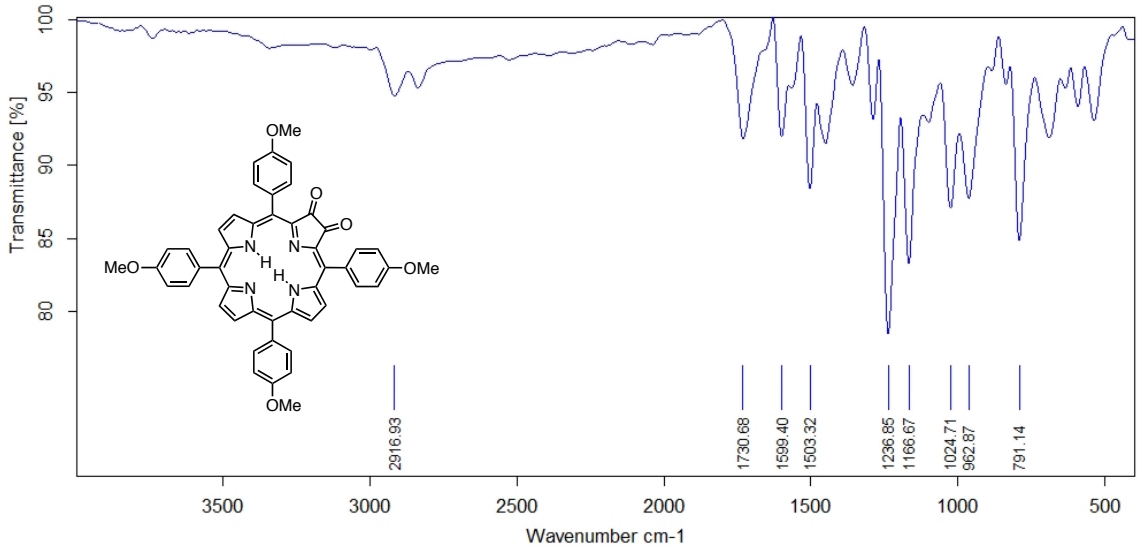

Figure S4. FT-IR spectrum (neat, diamond ATR) of **8**.

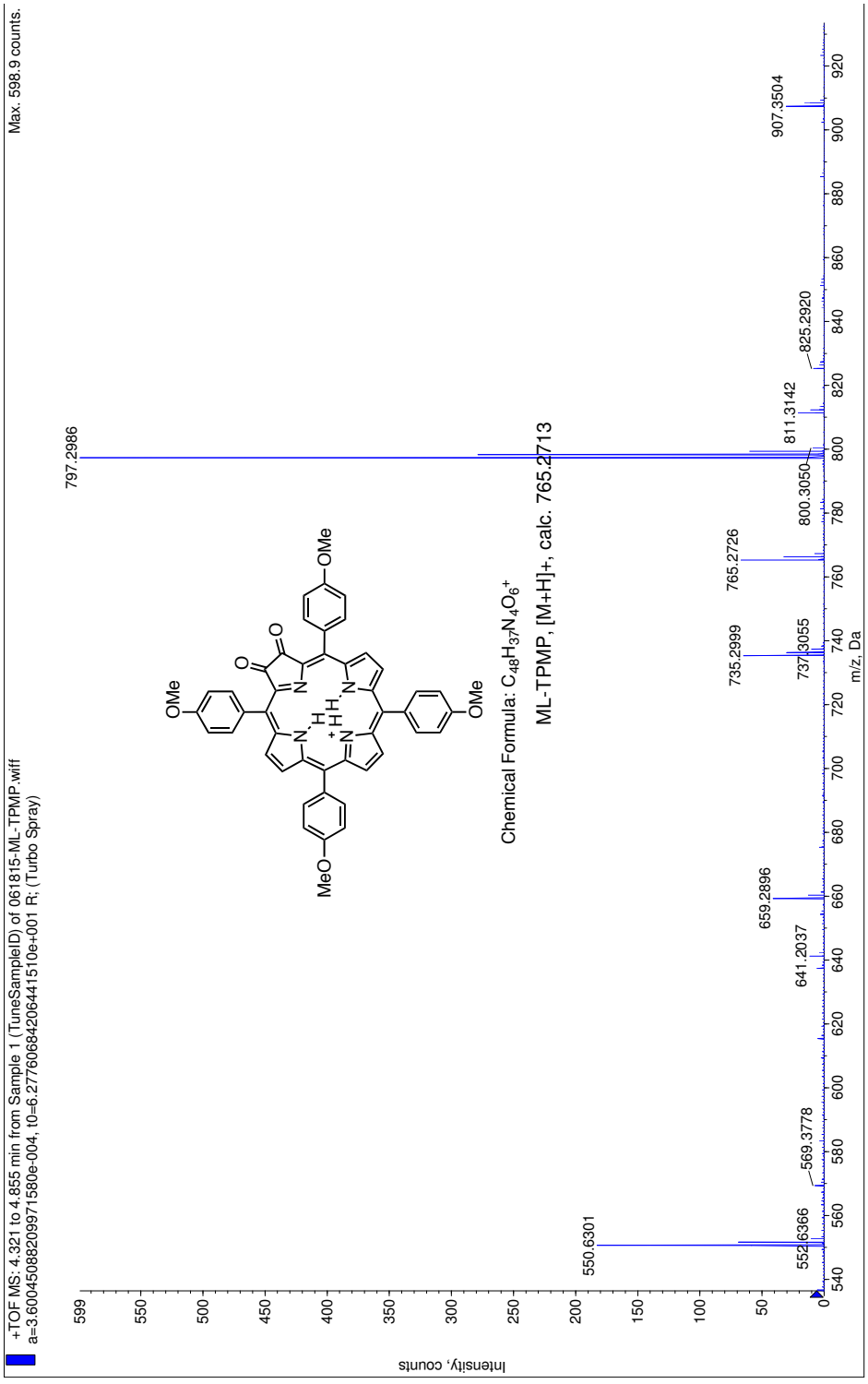

Figure S5. HR-MS (ESI$^+$, 100% CH_3CN, TOF) of **8**.

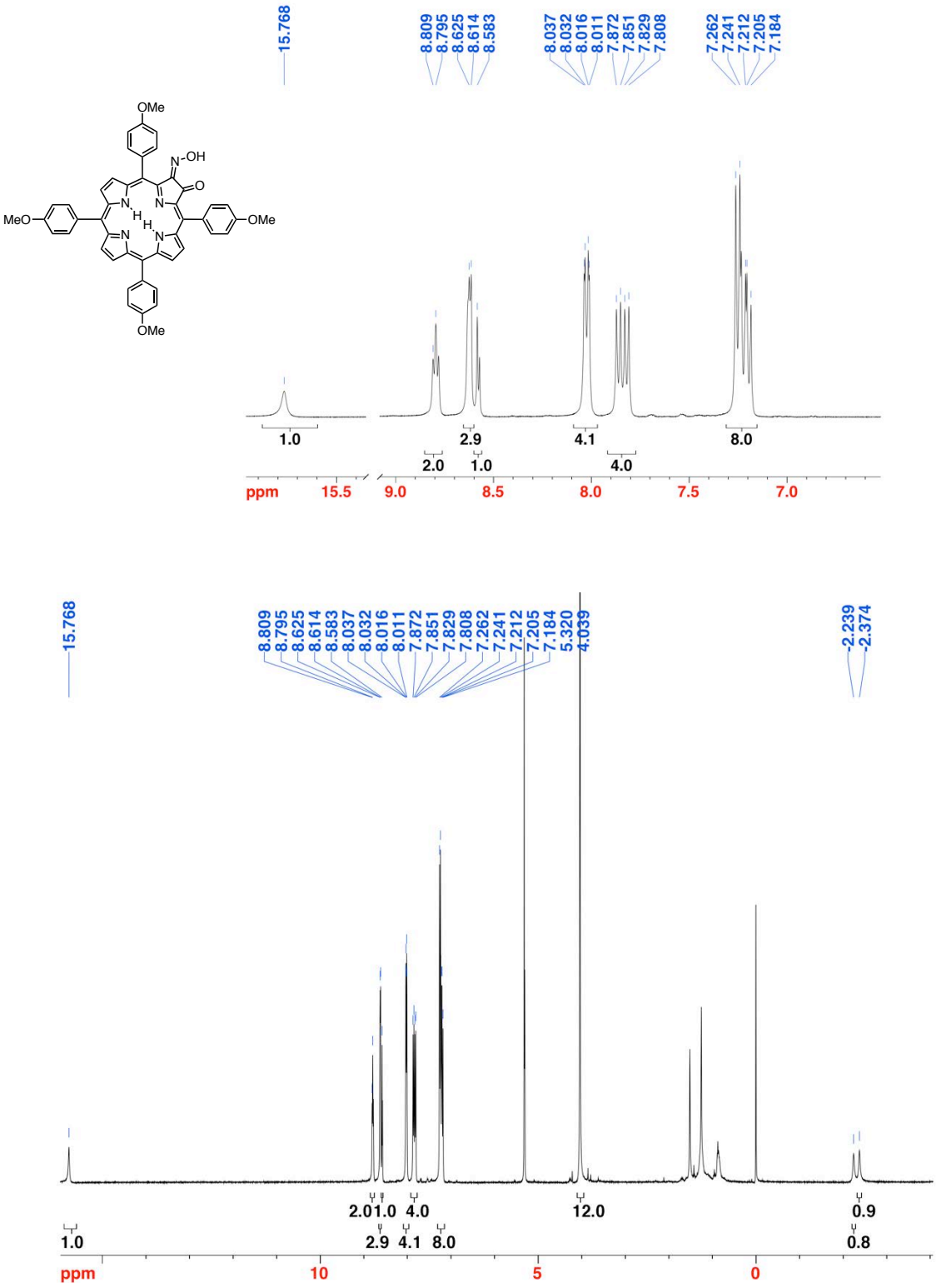

Figure S6. ^{1}H NMR spectrum (400 MHz, CD_2Cl_2) of **9**.

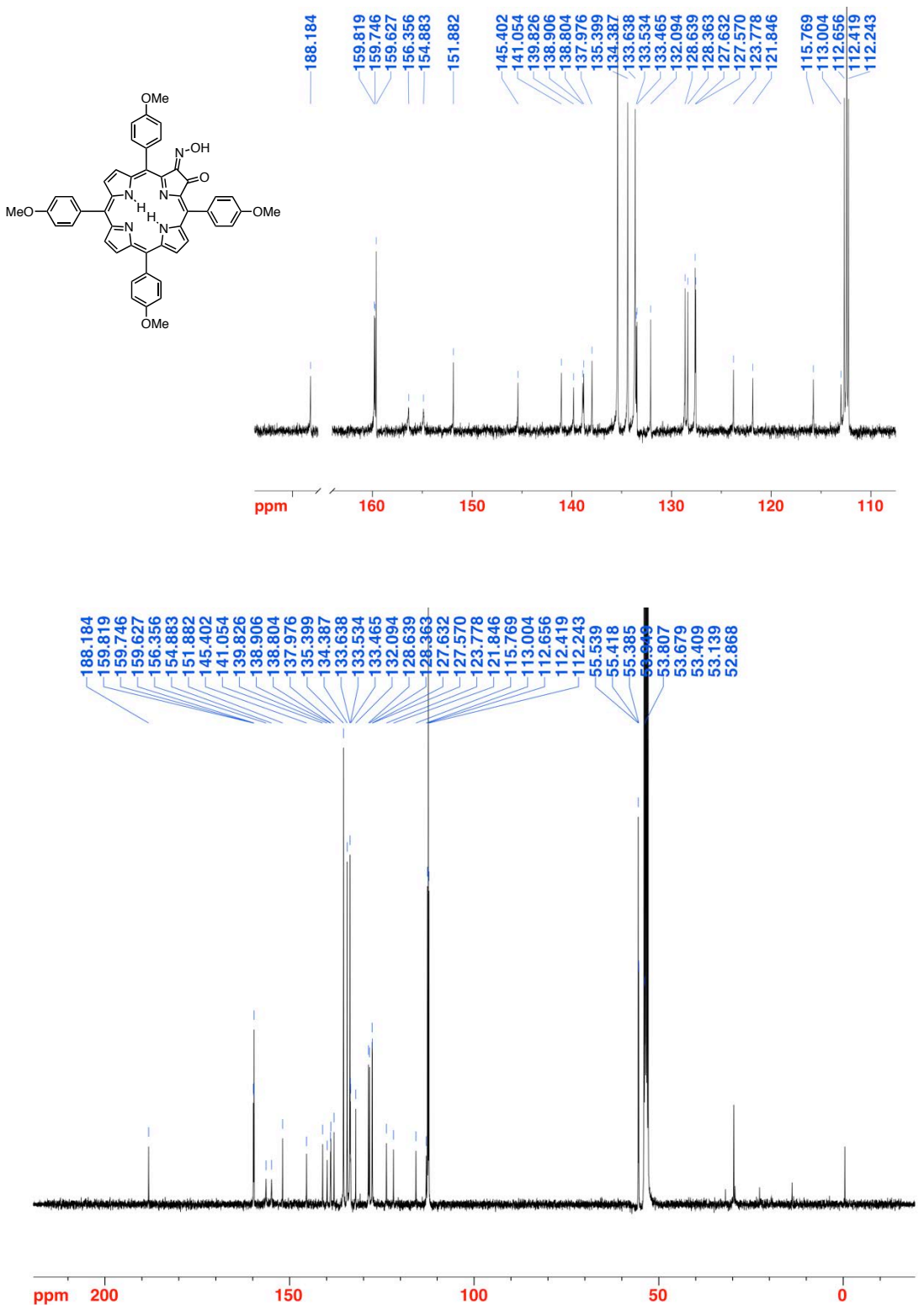

Figure S7. ^{13}C NMR spectrum (100 MHz, CD_2Cl_2) of **9**.

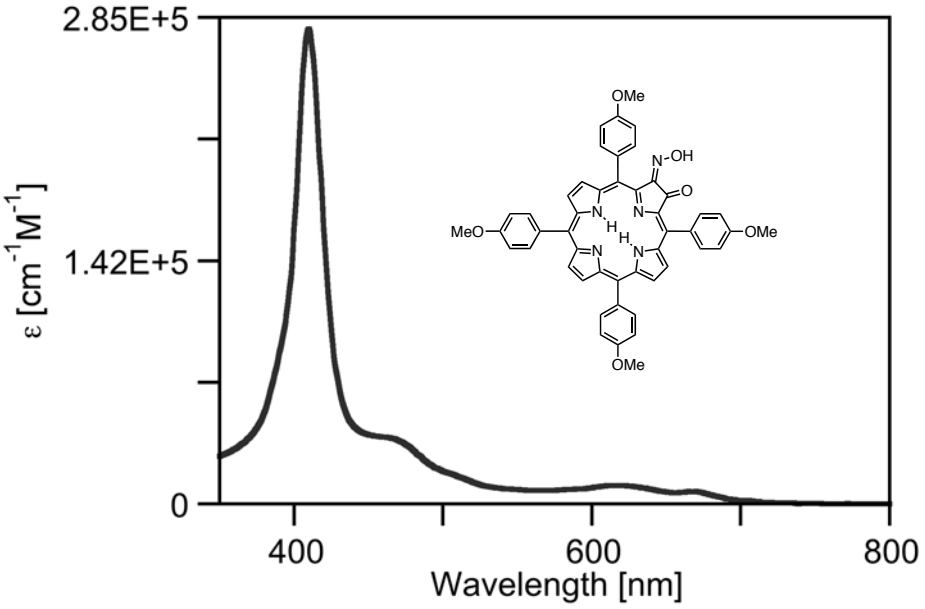

Figure S8. UV-vis spectrum (CH_2Cl_2) of **9**.

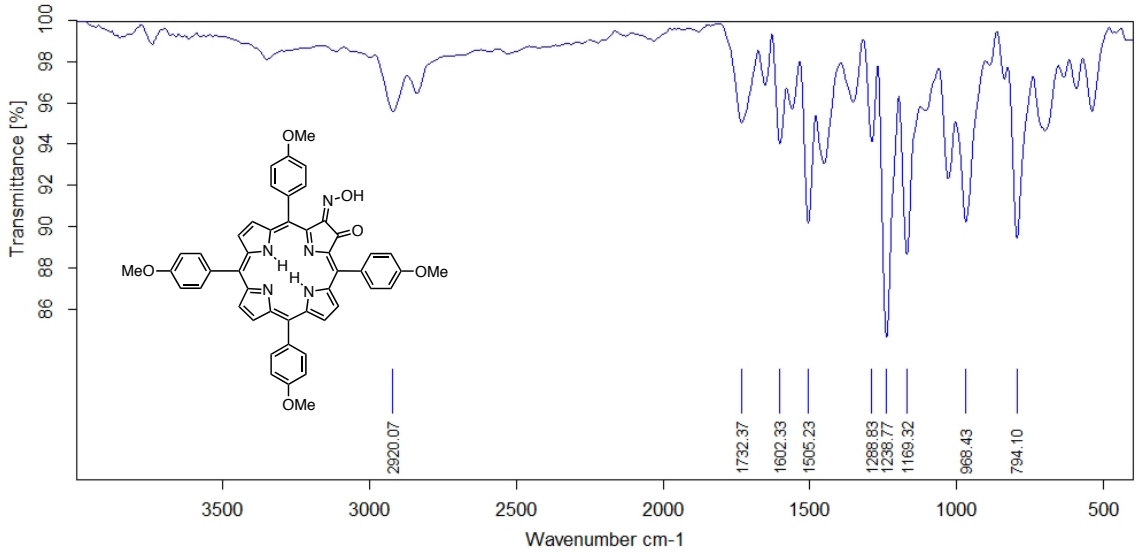

Figure S9. FT-IR spectrum (neat, diamond ATR) of **9**.

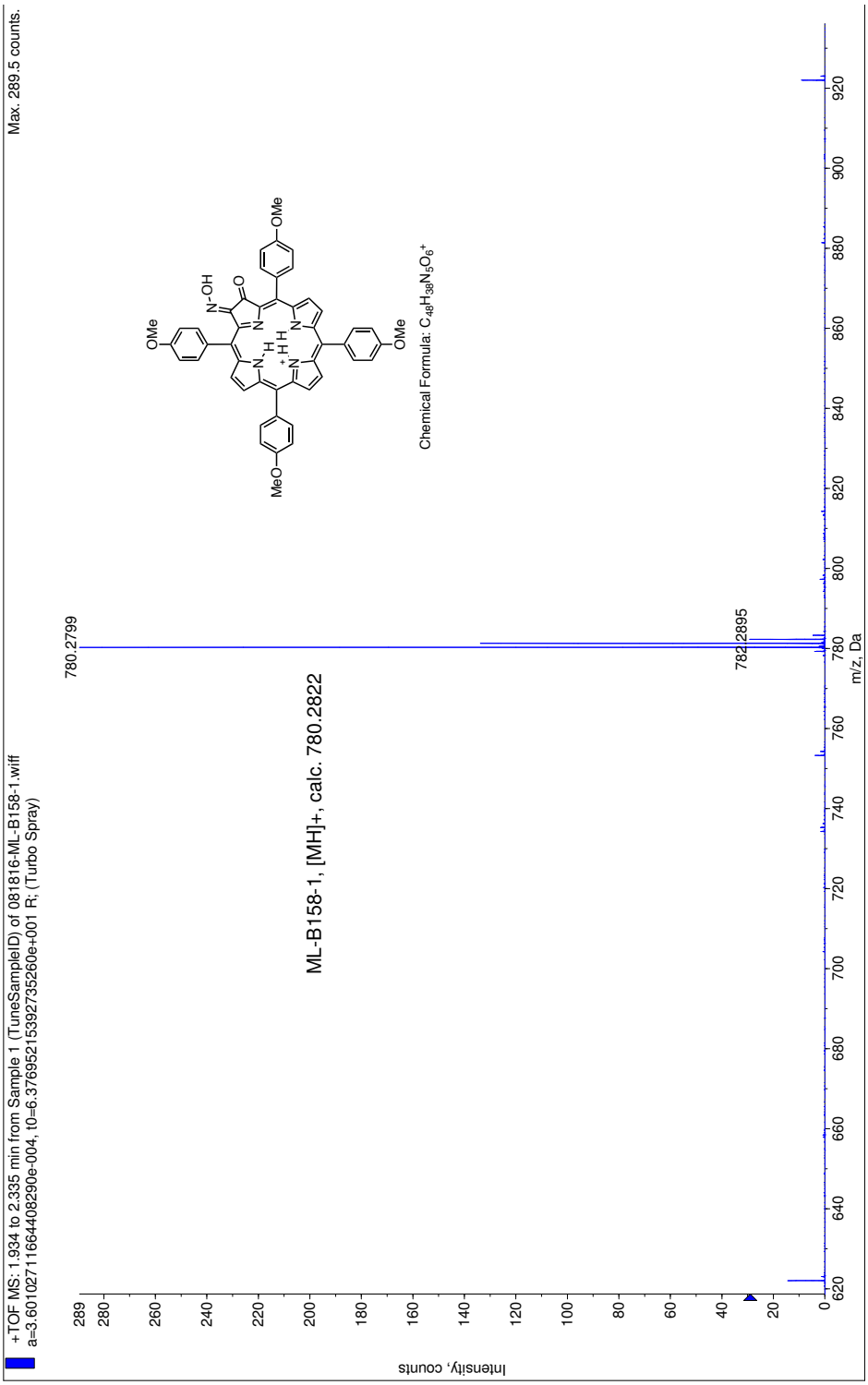

Figure S10. HR-MS (ESI^+, 100% CH_3CN, TOF) of **9**.

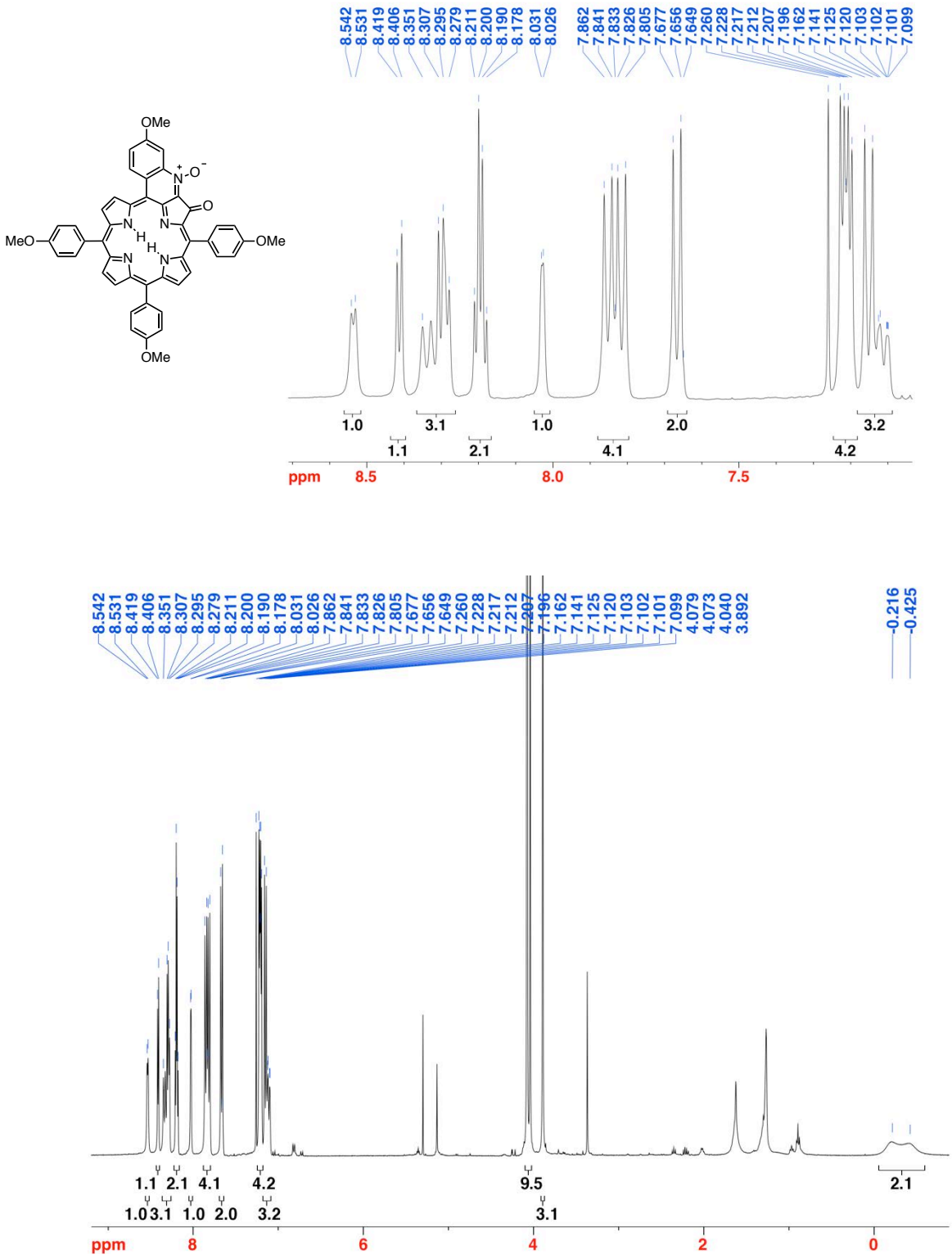

Figure S11. ^{1}H NMR spectrum (400 MHz, $CDCl_3$) of **5b**.

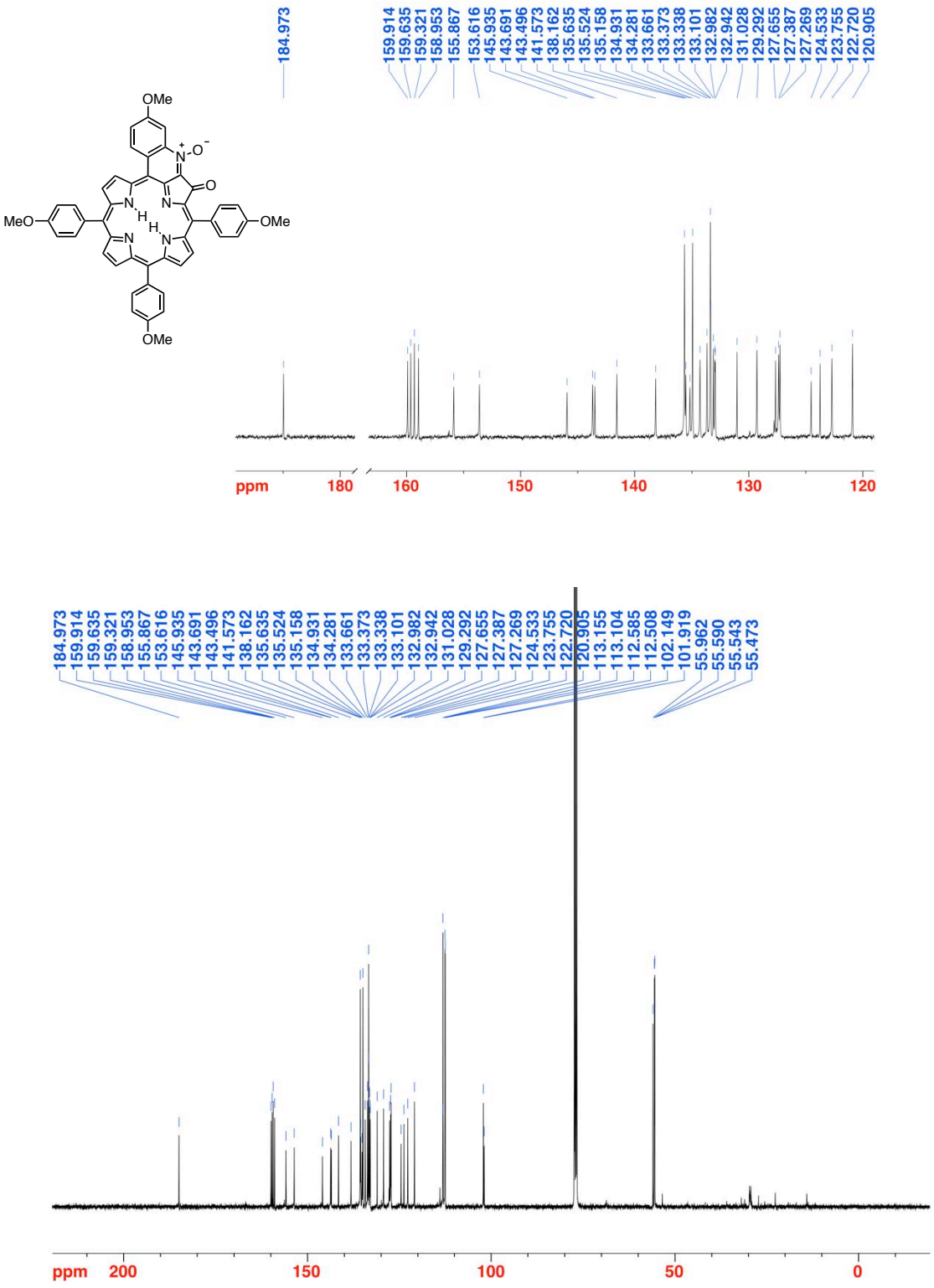

Figure S12. ^{13}C NMR spectrum (100 MHz, $CDCl_3$) of **5b**.

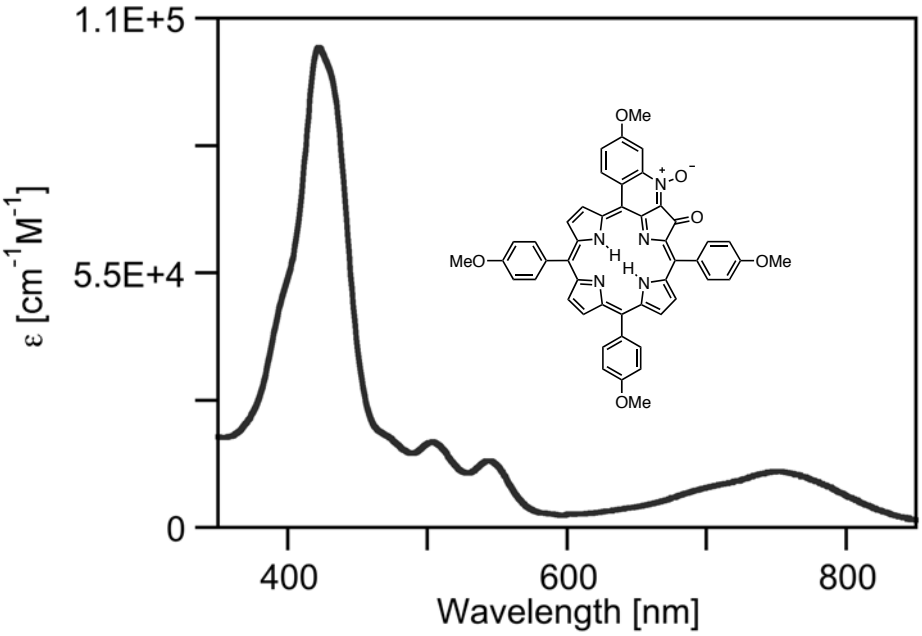

Figure S13. UV-vis spectrum (CH_2Cl_2) of **5b**.

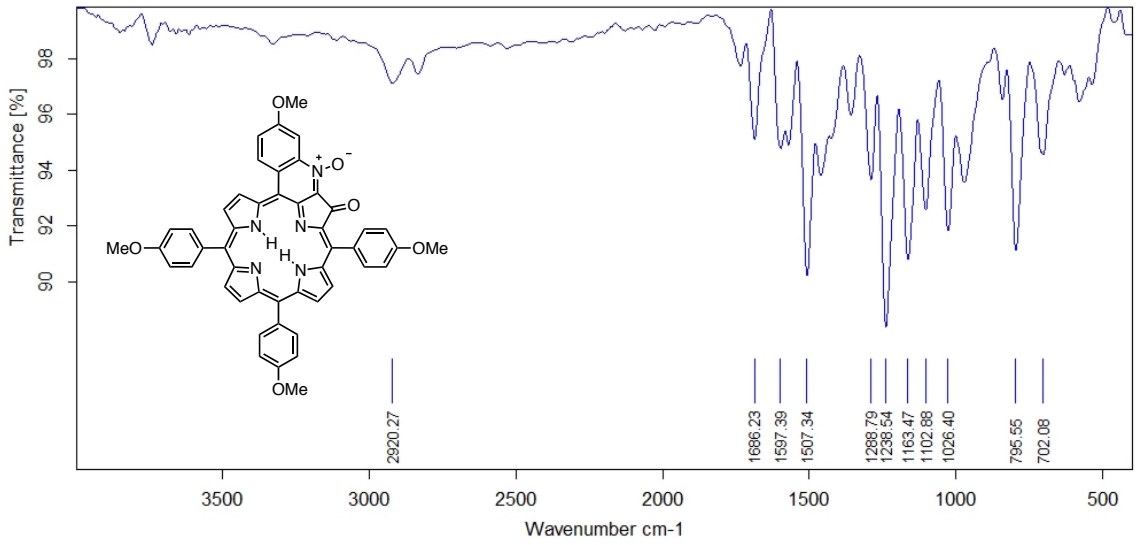

Figure S14. FT-IR spectrum (neat, diamond ATR) of **5b**.

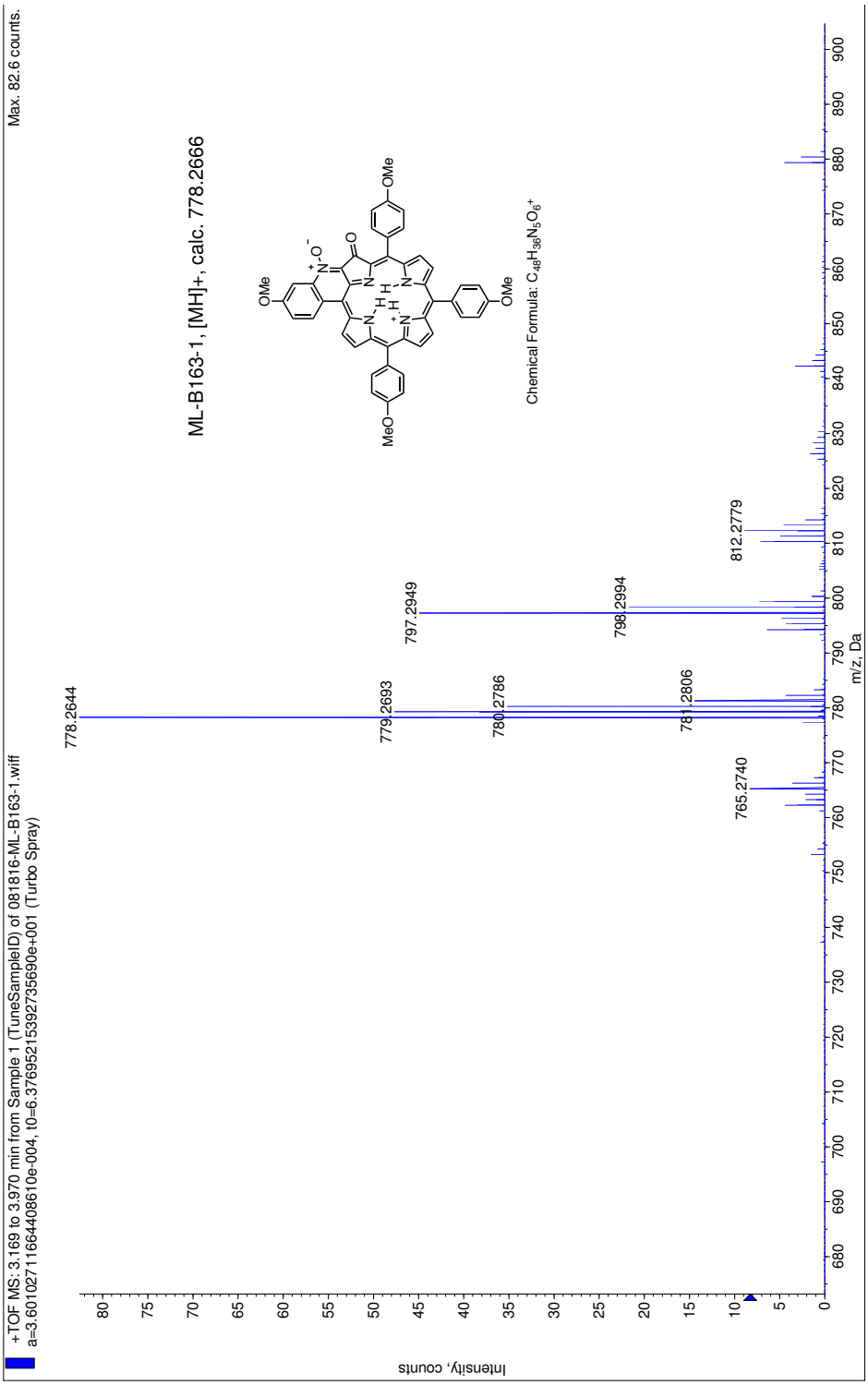

Figure S15. HR-MS (ESI^+, 100% CH_3CN, TOF) of **5b**.

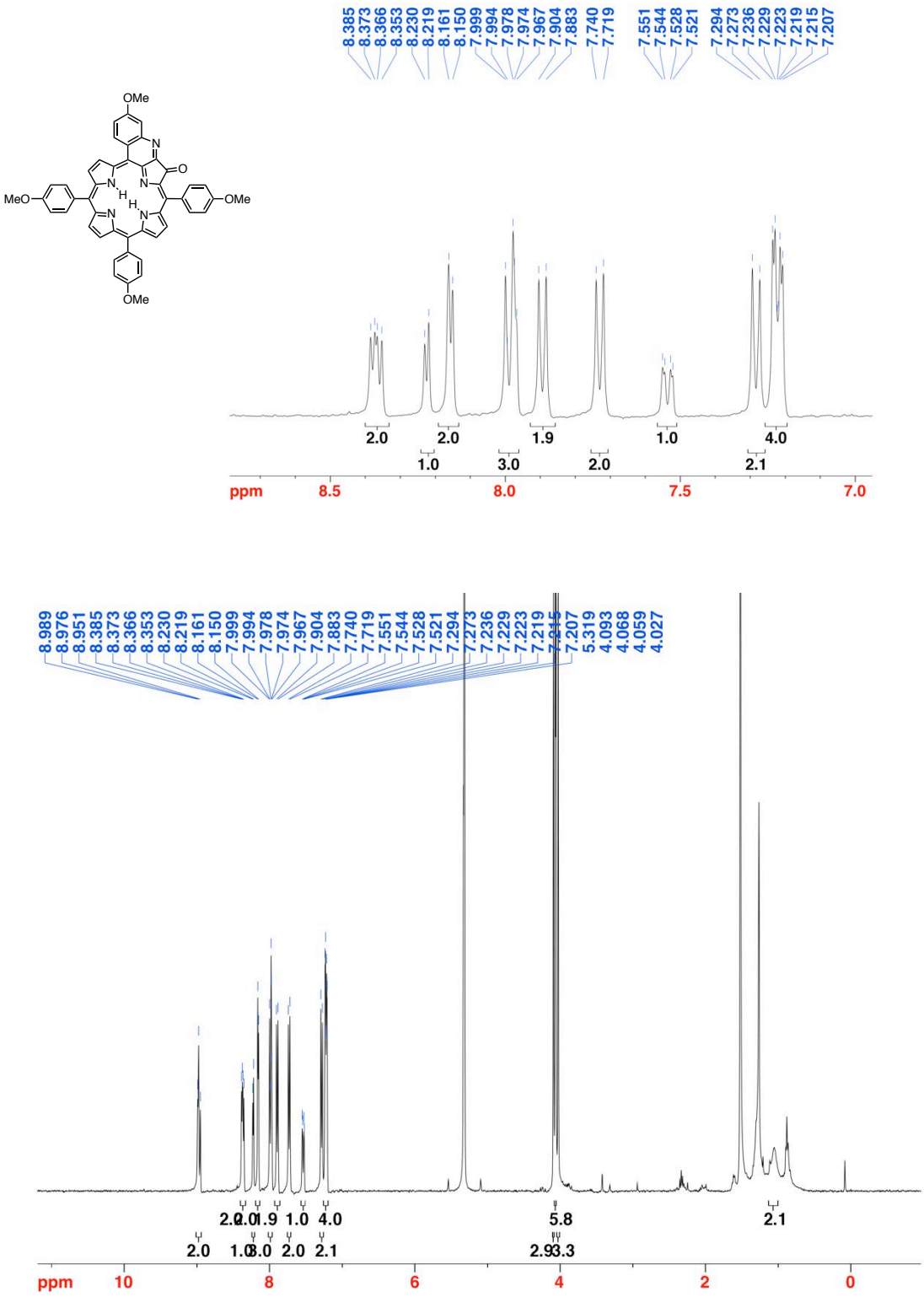

Figure S16. ^{1}H NMR spectrum (400 MHz, CD_2Cl_2) of **4b**.

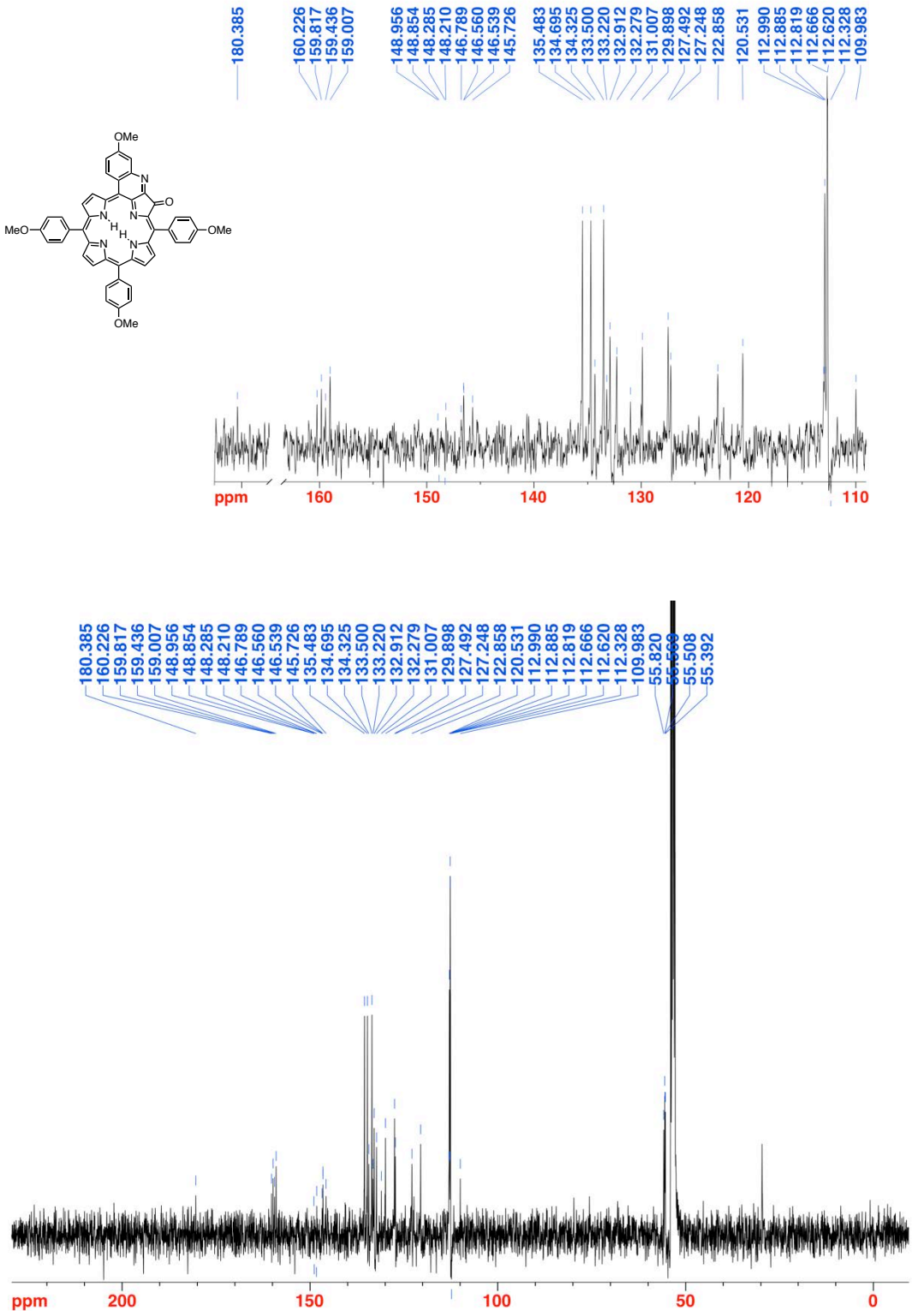

Figure S17. ^{13}C NMR spectrum (100 MHz, CD_2Cl_2) of **4b** (the compound has limited solubility).

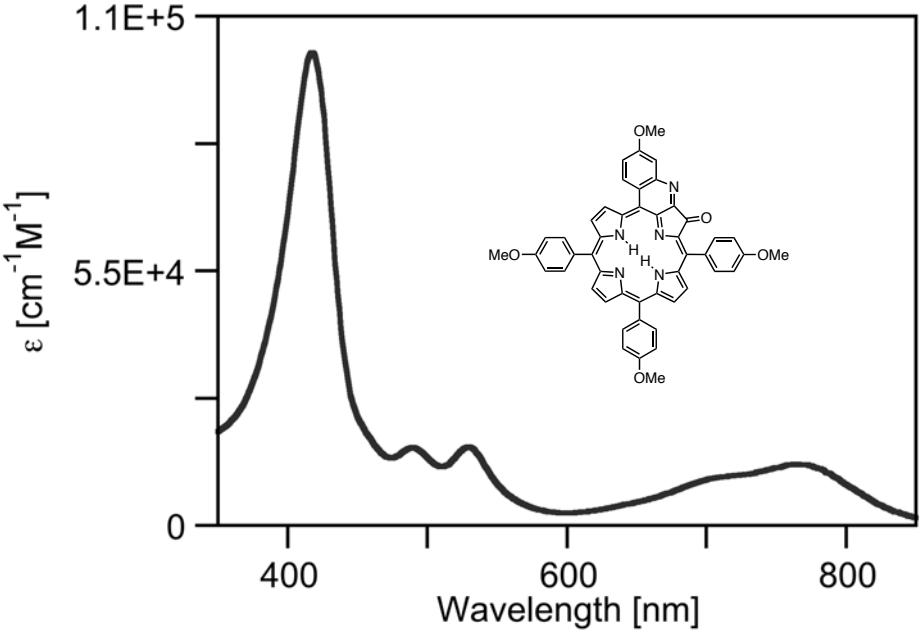

Figure S18. UV-vis spectrum (CH_2Cl_2) of **4b**.

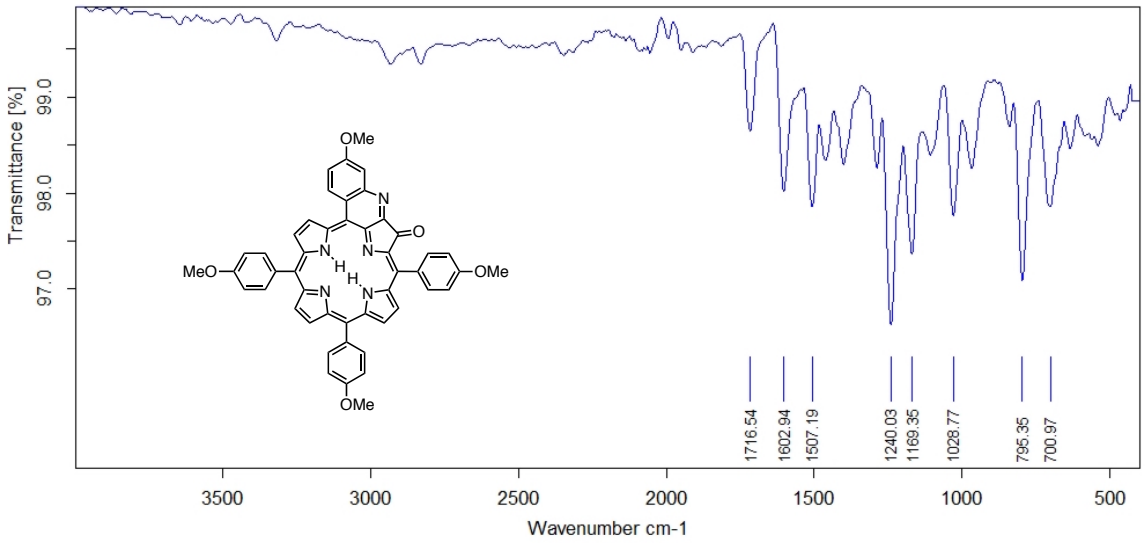

Figure S19. FT-IR spectrum (neat, diamond ATR) of **4b**.

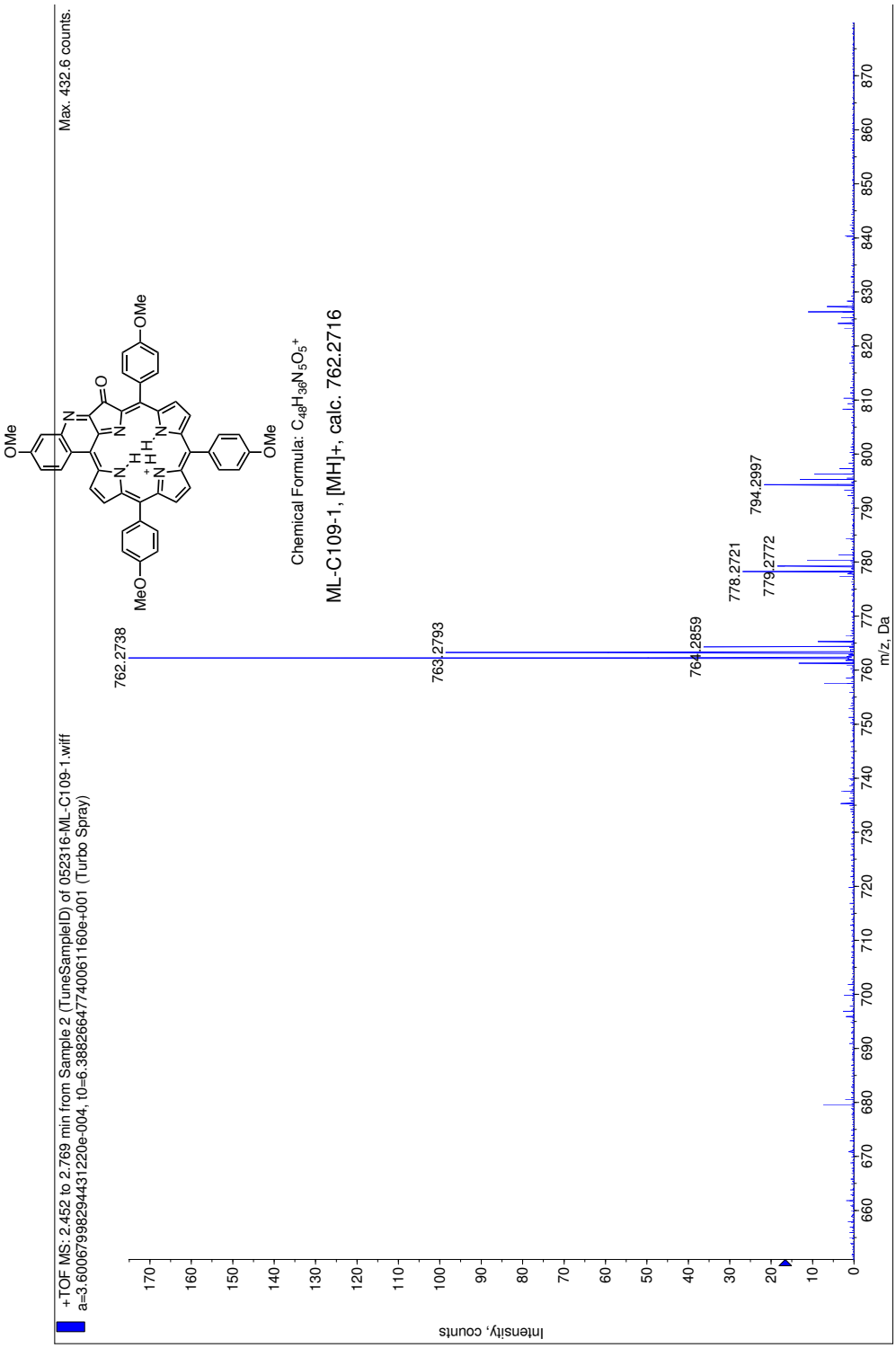

Figure S20. HR-MS (ESI^+, 100% CH_3CN, TOF) of **4b**.

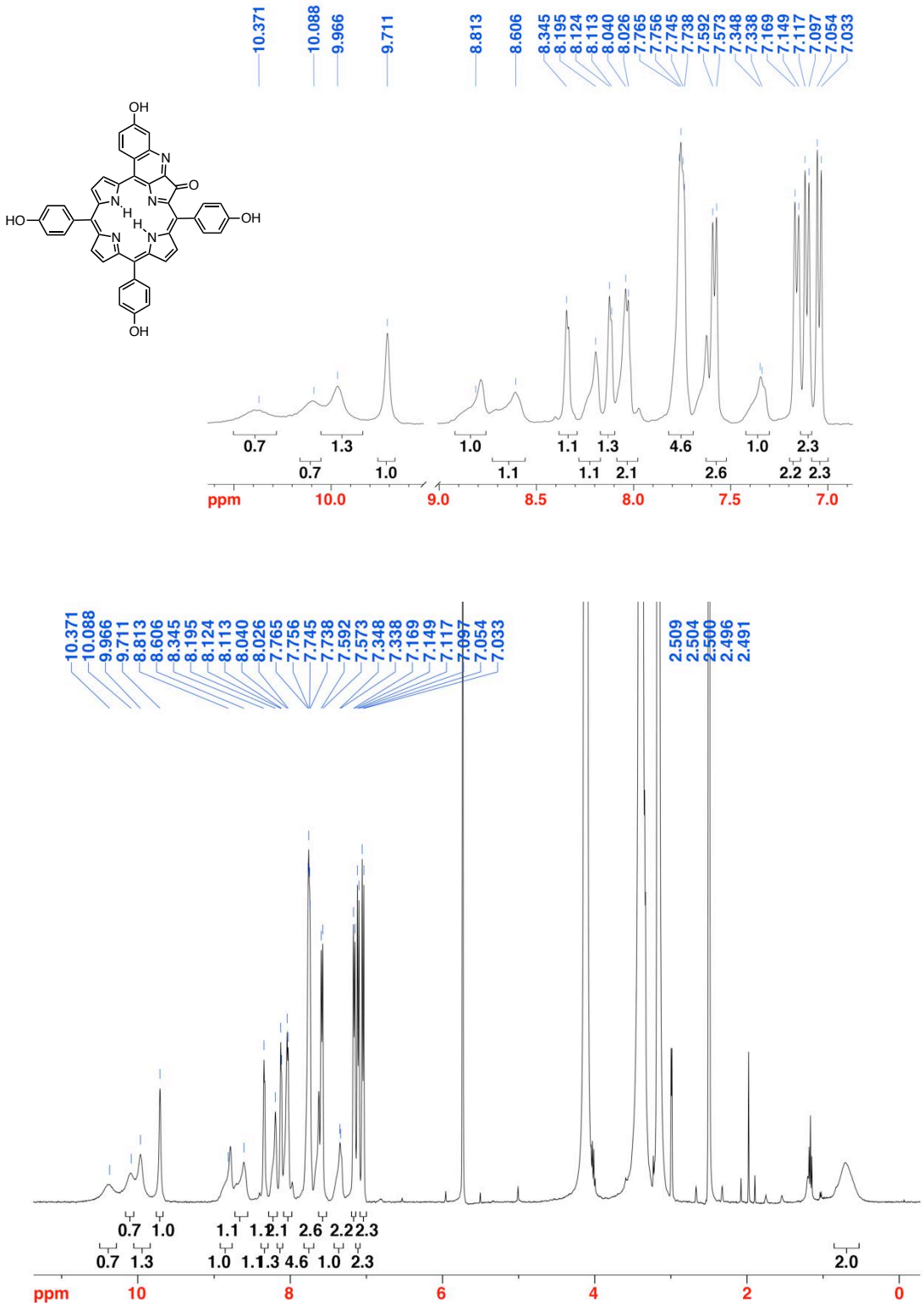

Figure S21. ^{1}H NMR spectrum (400 MHz, DMSO-d_6) of **4c**.

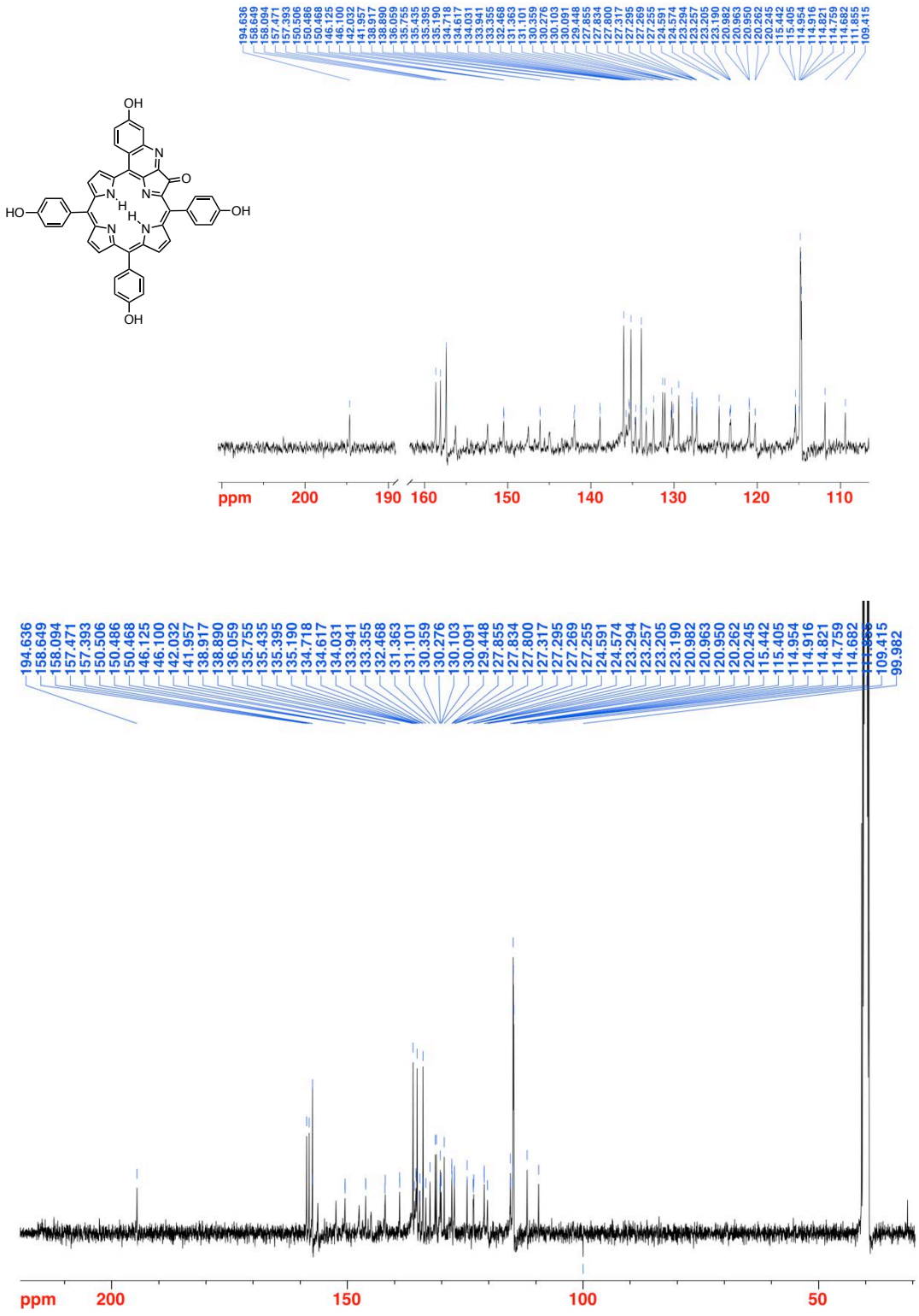

Figure S22. ^{13}C NMR spectrum (100 MHz, DMSO-d_6) of **4c**.

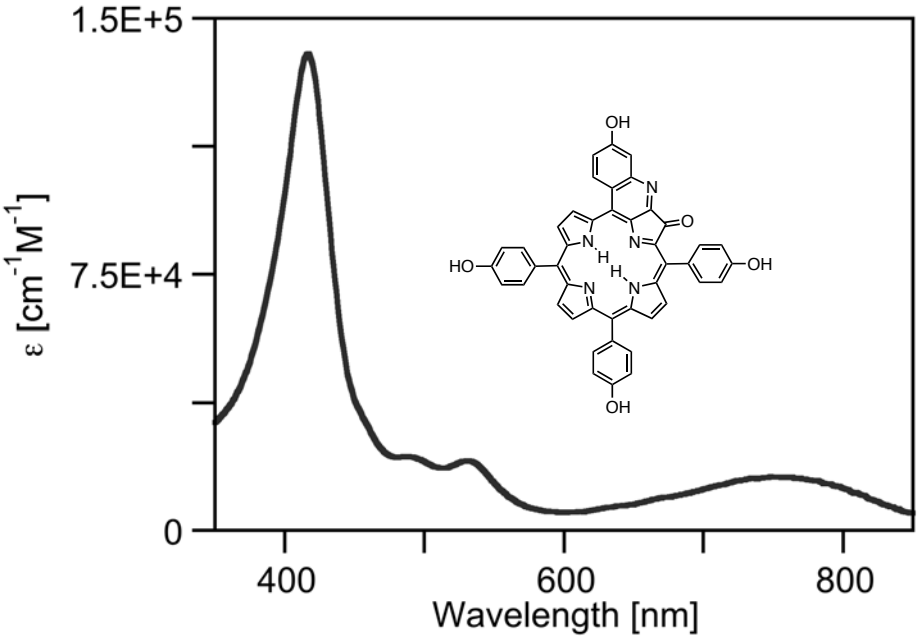

Figure S23. UV-vis spectrum (MeOH) of **4c**.

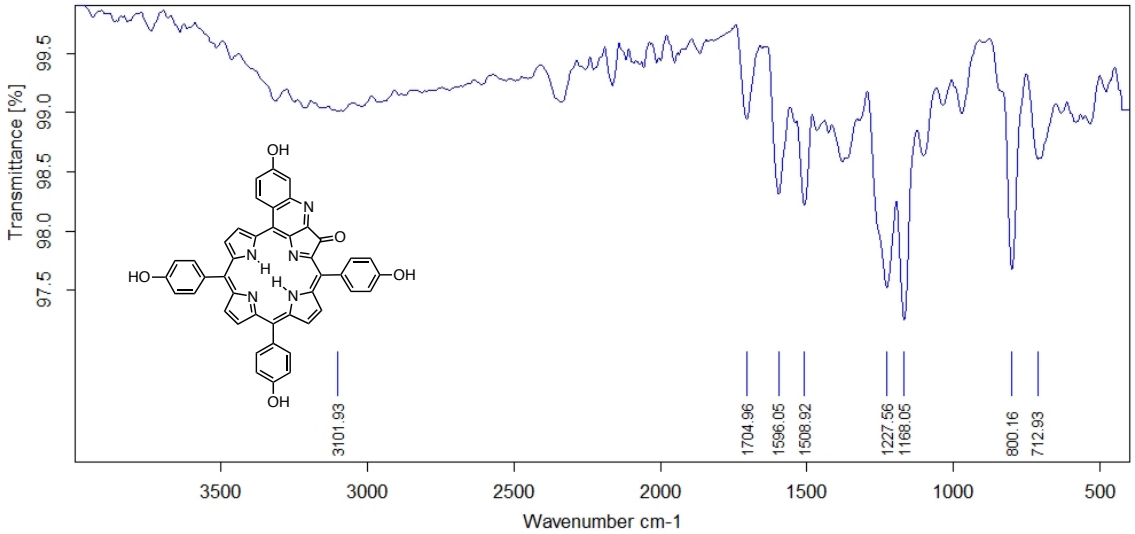

Figure S24. FT-IR spectrum (neat, diamond ATR) of **4c**.

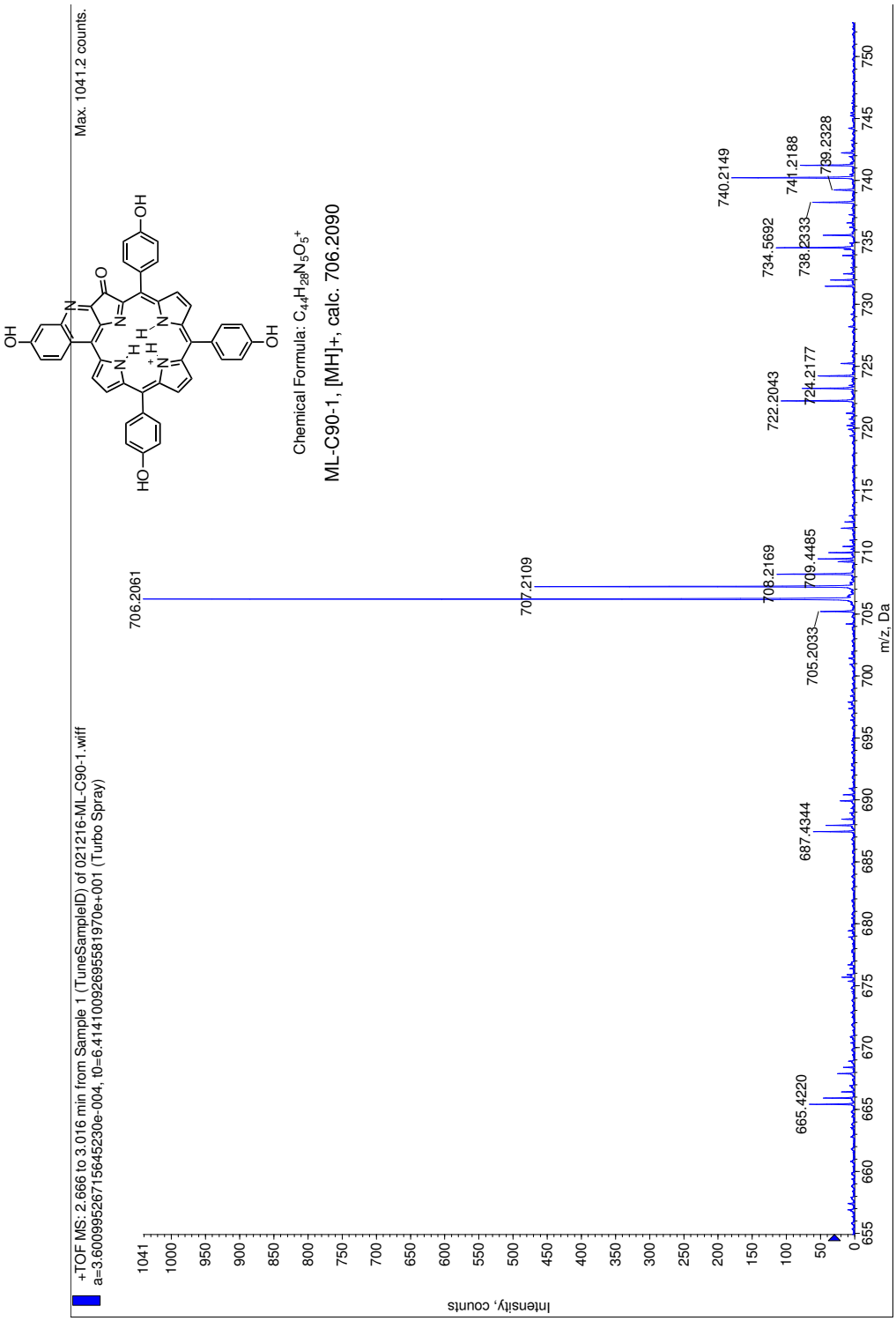

Figure S25. HR-MS (ESI^+, 100% CH_3CN, TOF) of **4c**.

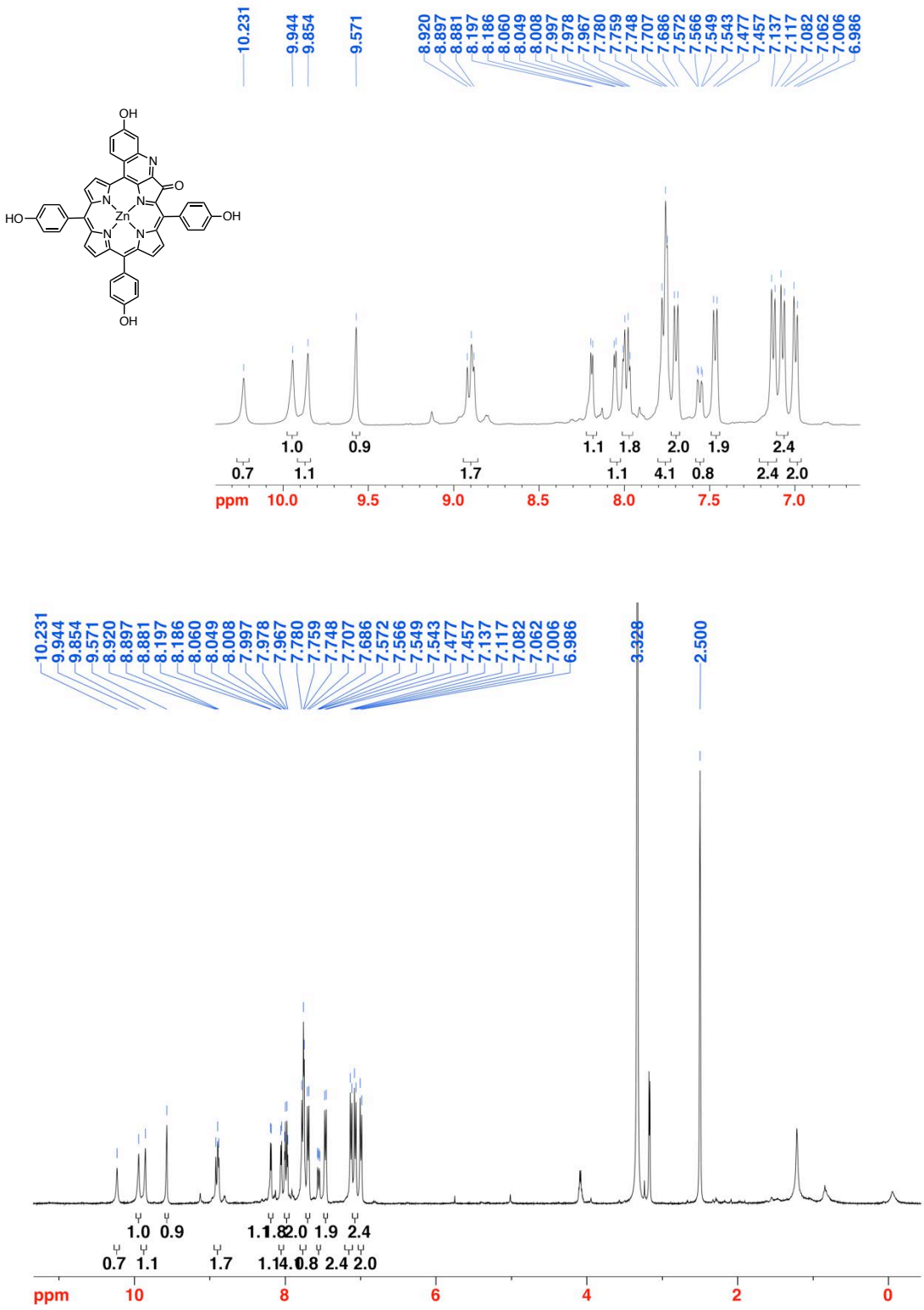

Figure S26. ^{1}H NMR spectrum (400 MHz, DMSO-d_6) of **4c^{Zn}**.

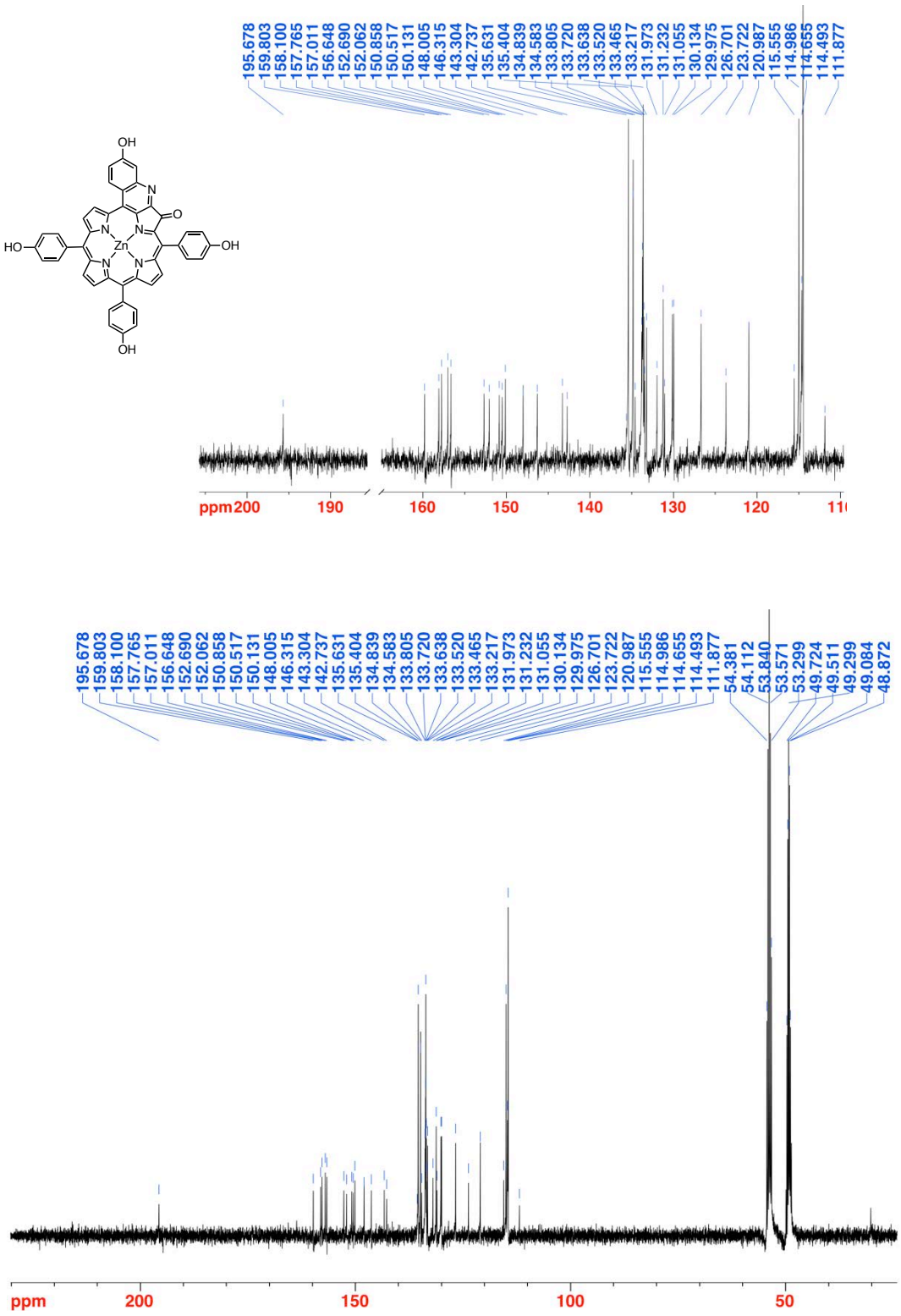

Figure S27. ^{13}C NMR spectrum (100 MHz, CD_2Cl_2/10% MeOD) of **4c^{Zn}**.

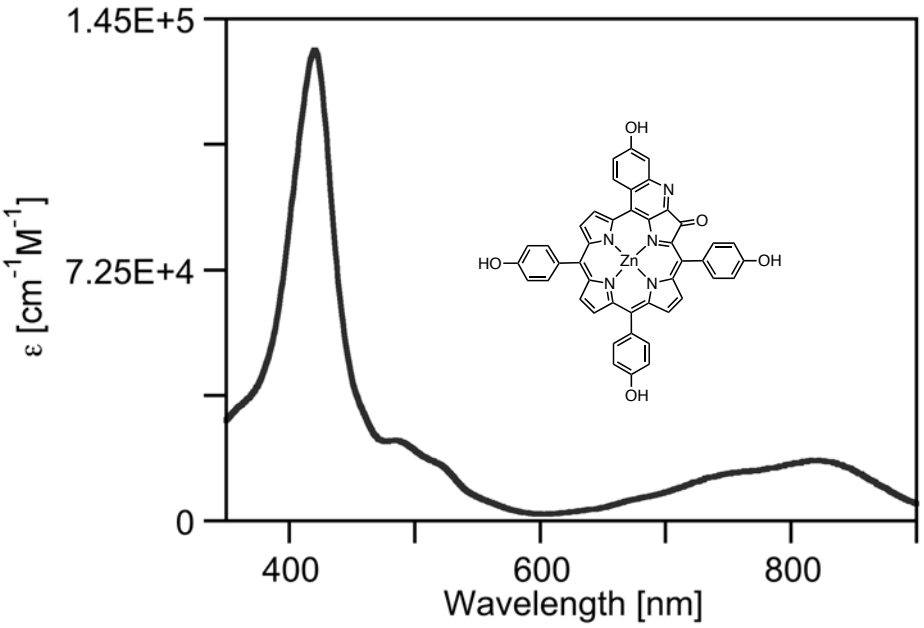

Figure S28. UV-vis spectrum (MeOH) of **4c^{Zn}**.

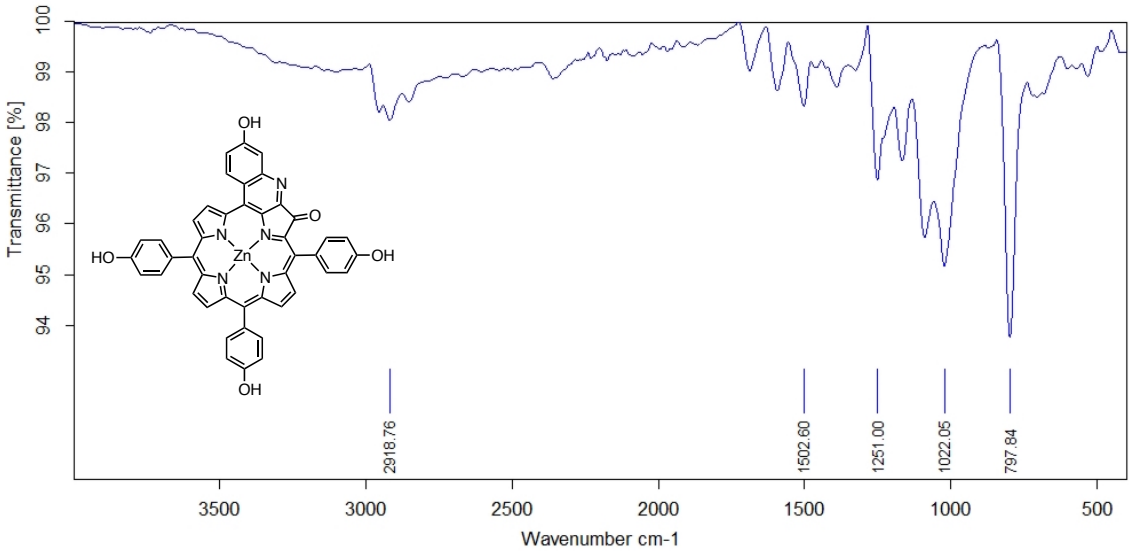

Figure S29. FT-IR spectrum (neat, diamond ATR) of **4c^{Zn}**.

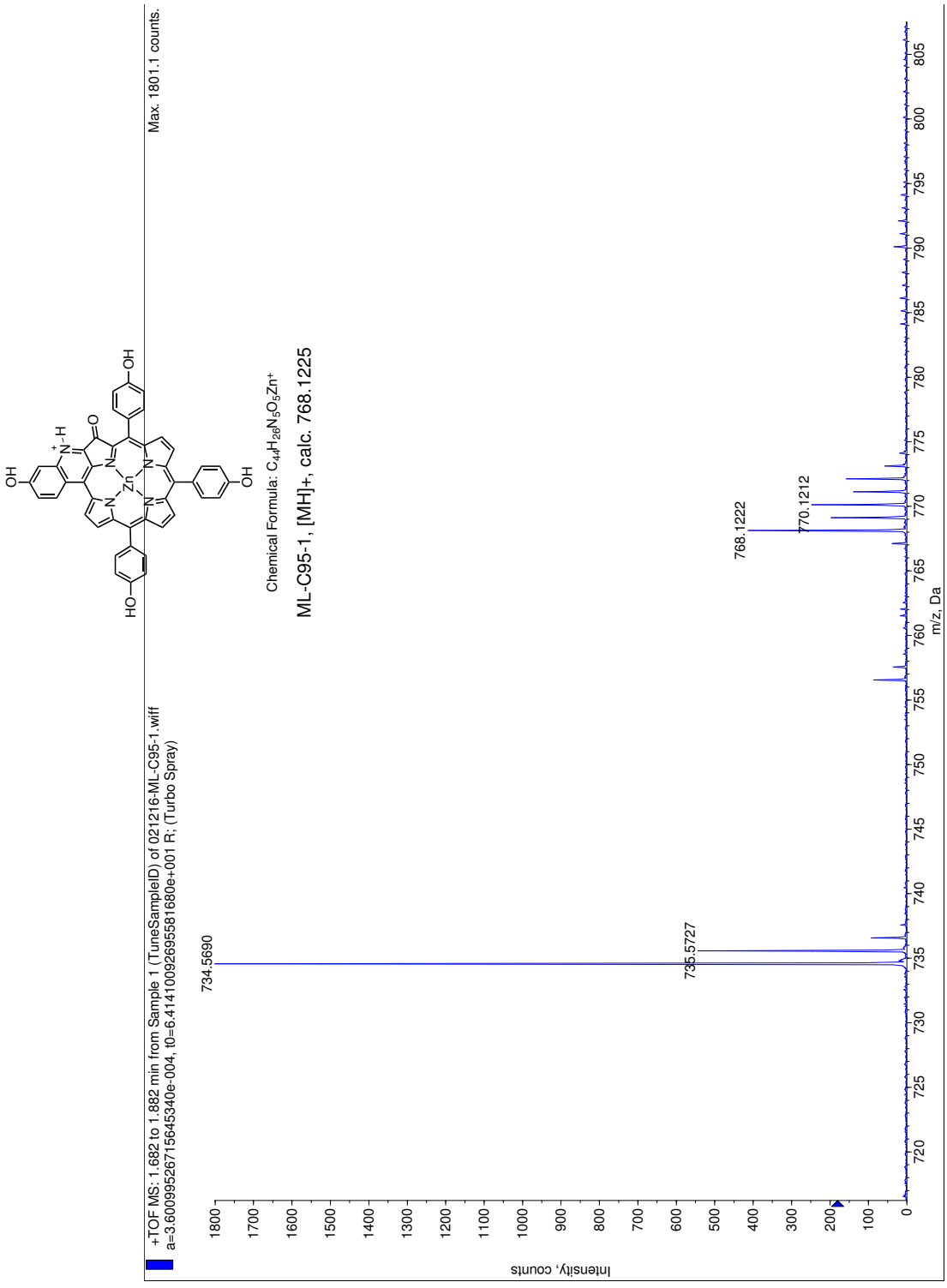

Figure S30. HR-MS (ESI$^+$, 100% CH_3CN, TOF) of **4c^{Zn}**.

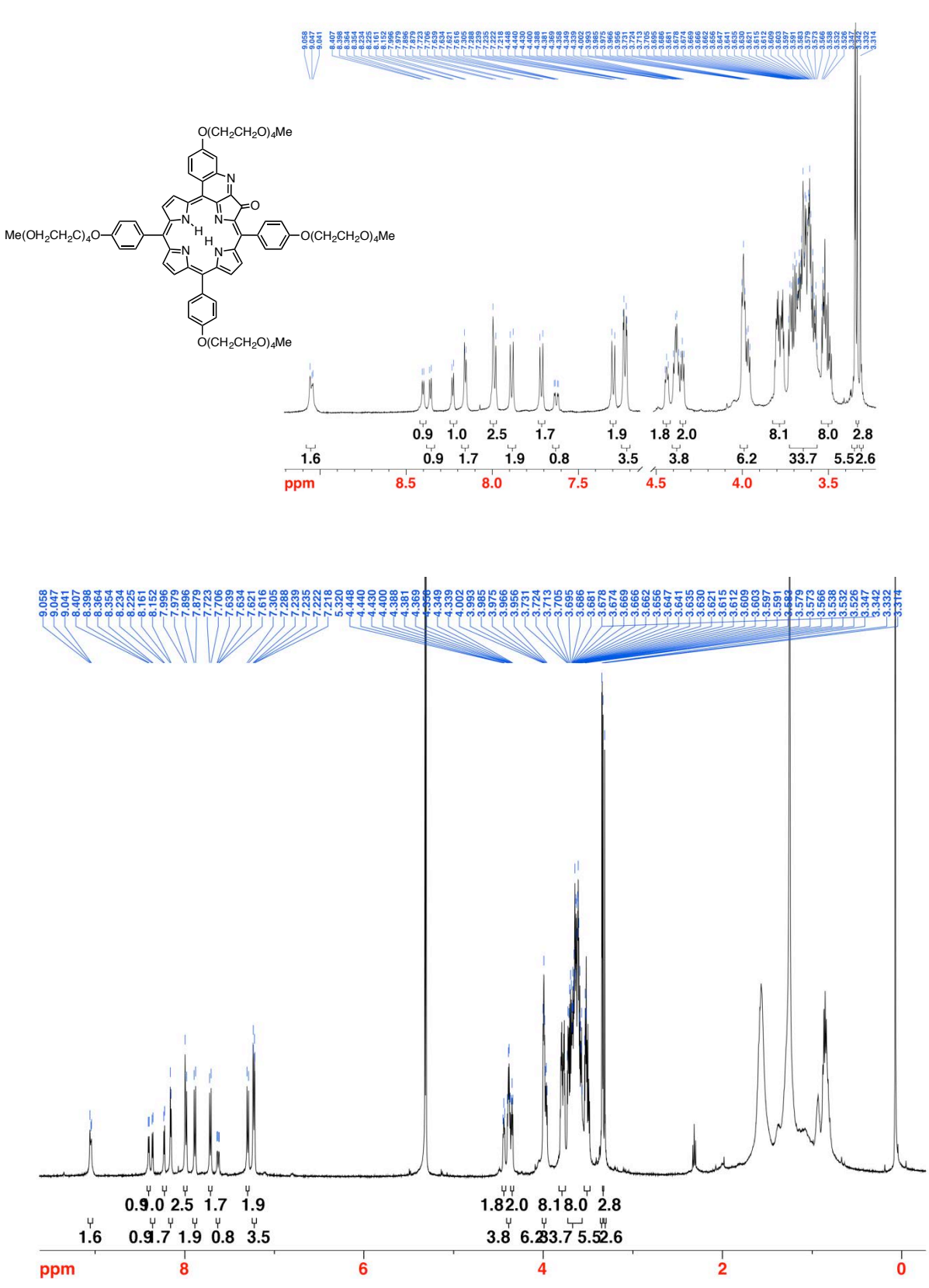

Figure S31. ^{1}H NMR spectrum (500 MHz, CD_2Cl_2) of **4d**.

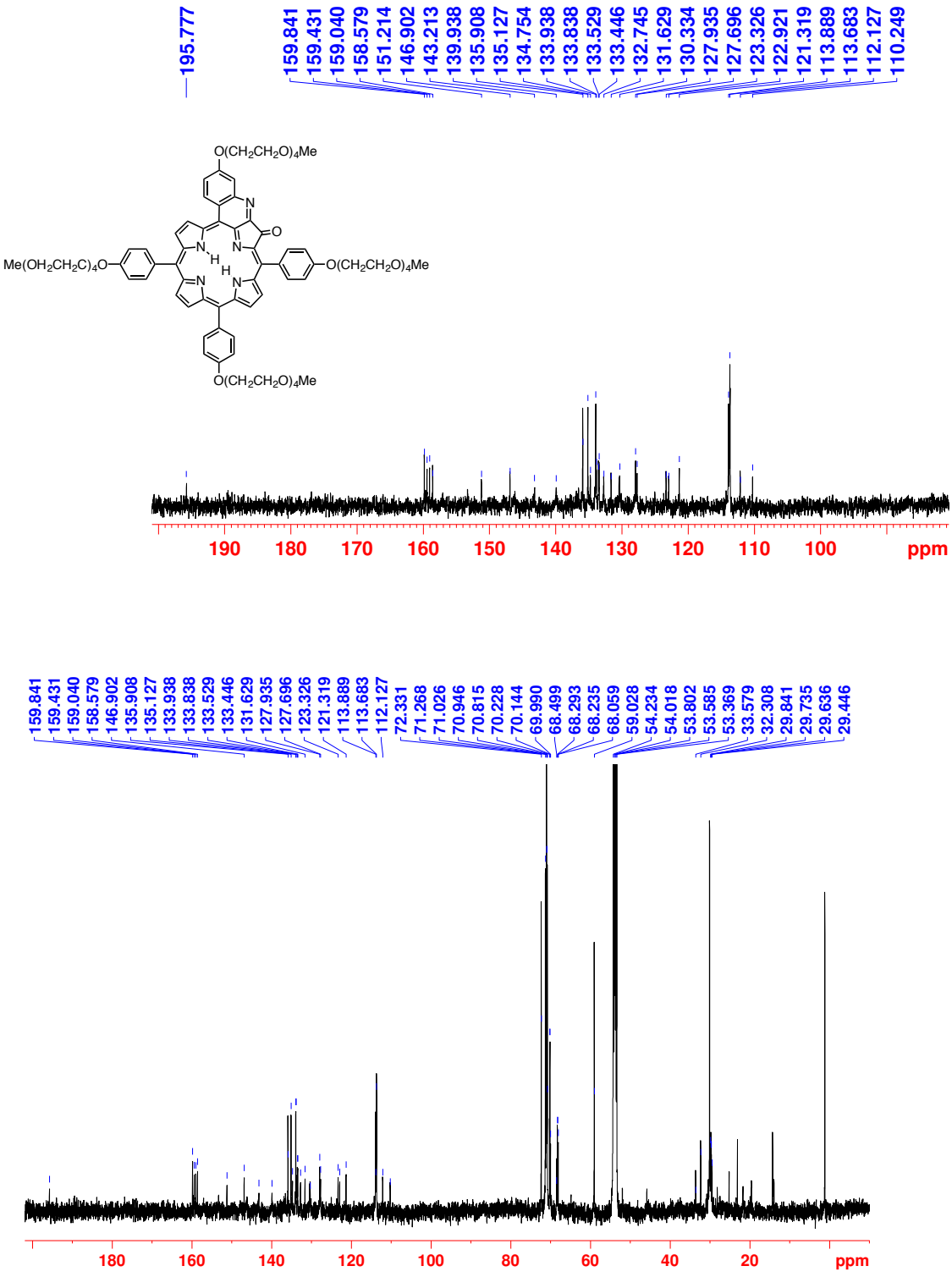

Figure S32. ^{13}C NMR spectrum (125 MHz, CD_2Cl_2) of **4d**.

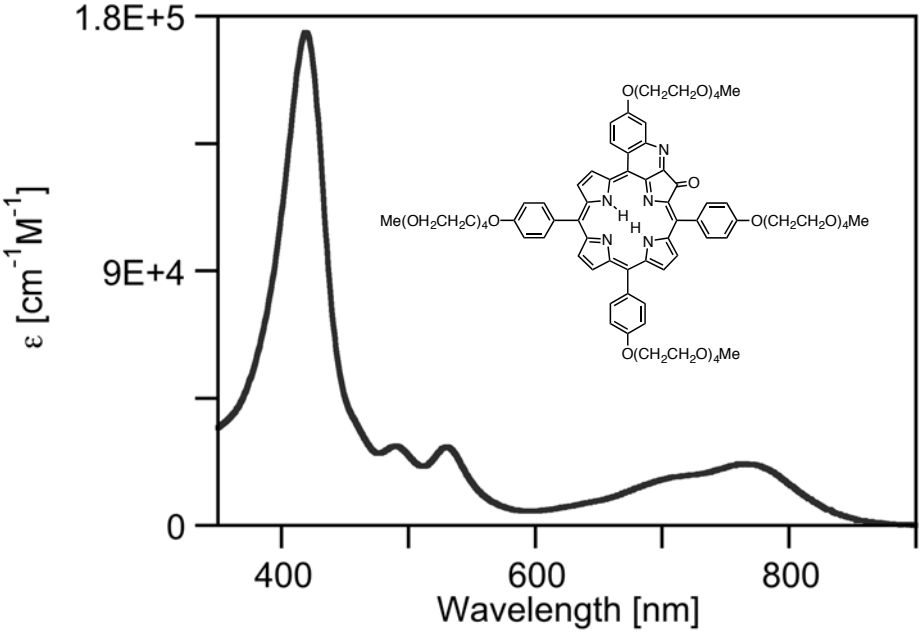

Figure S33. UV-vis spectrum (CH_2Cl_2) of **4d**.

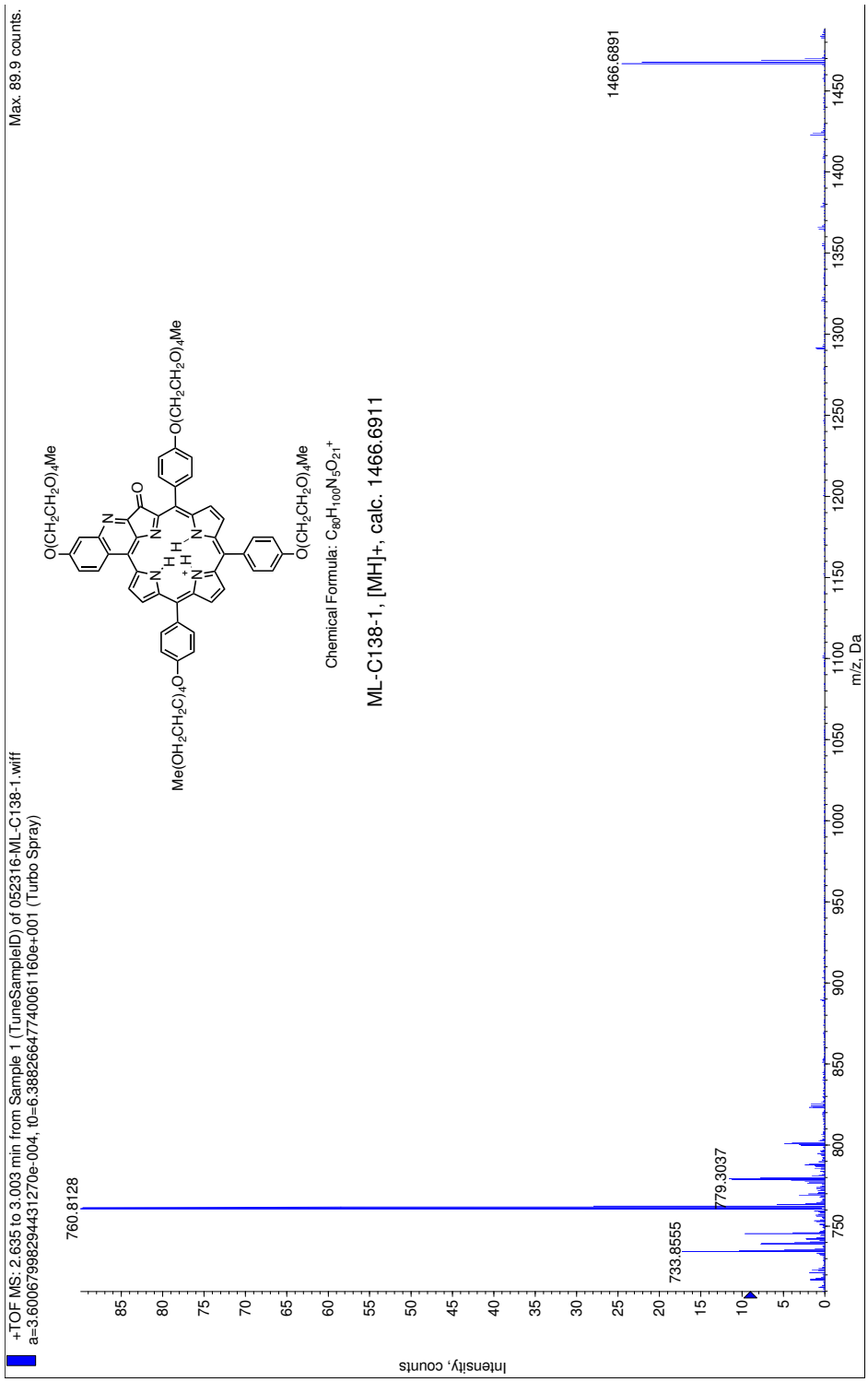

Figure S34. HR-MS (ESI^+, 100% CH_3CN, TOF) of **4d**.

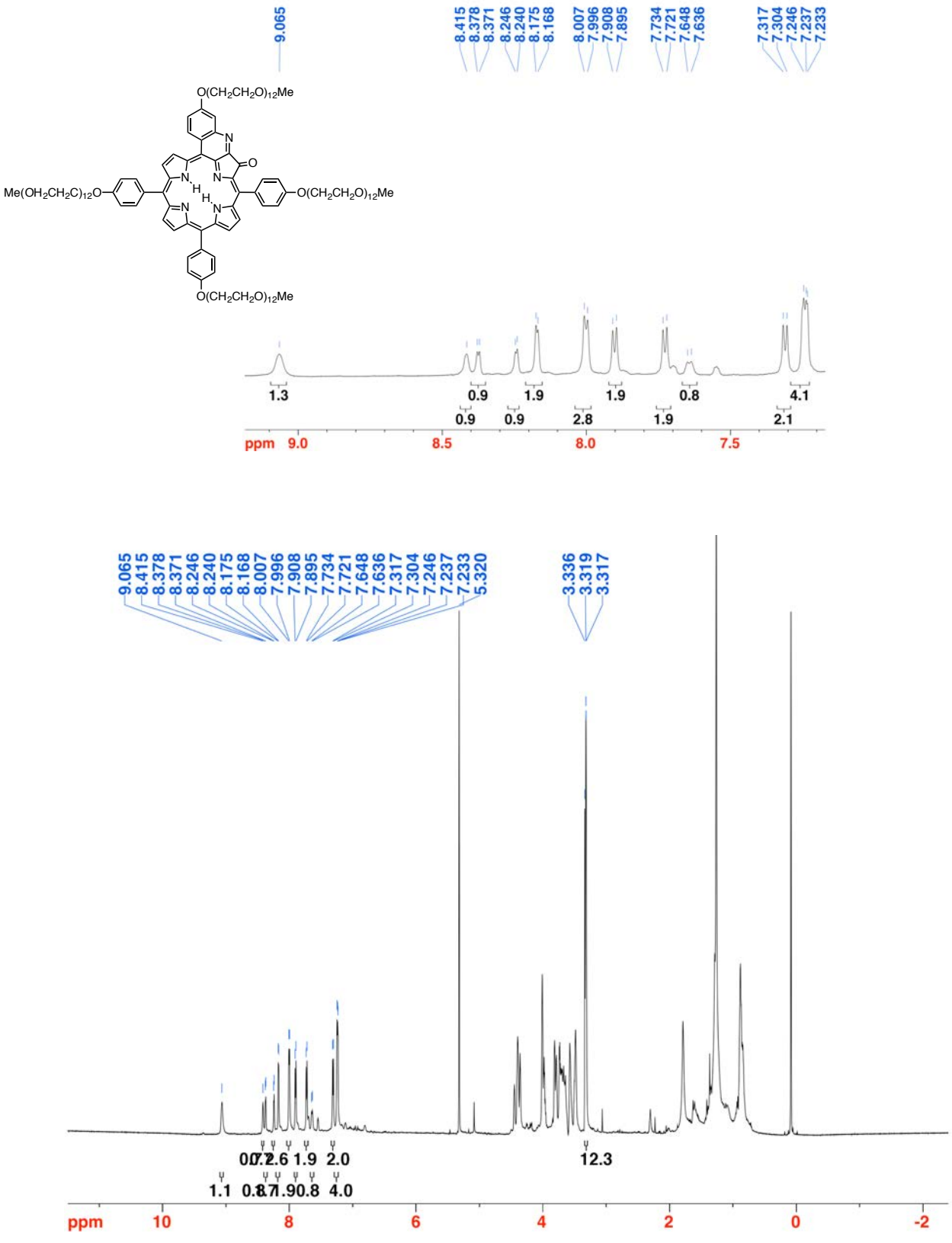

Figure S35. ^{1}H NMR spectrum (400 MHz, CD_2Cl_2) of **4e**.

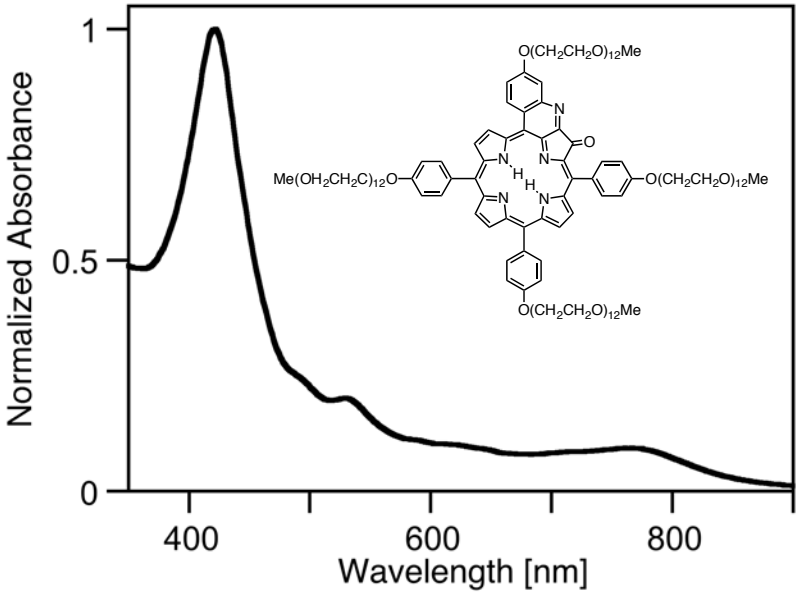

Figure S36. UV-vis spectrum (H_2O) of **4e**.

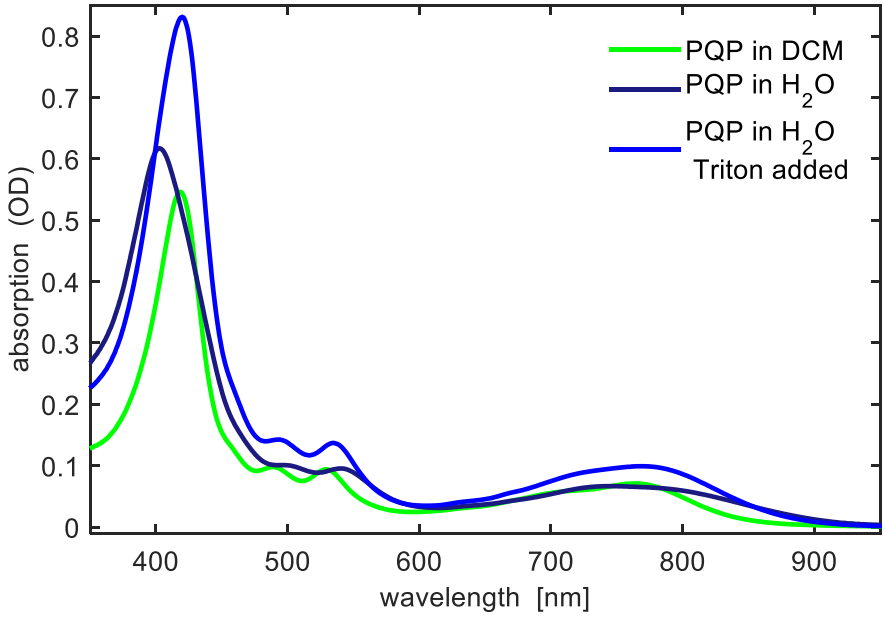

Figure S37. Absorption spectra of **4e** (PQP) in CH_2Cl_2, H_2O and H_2O-Triton-X solutions. The change of the absorption spectrum of **4e** in H_2O after adding triton indicates that **4e** is somewhat aggregated in pure aqueous solution.

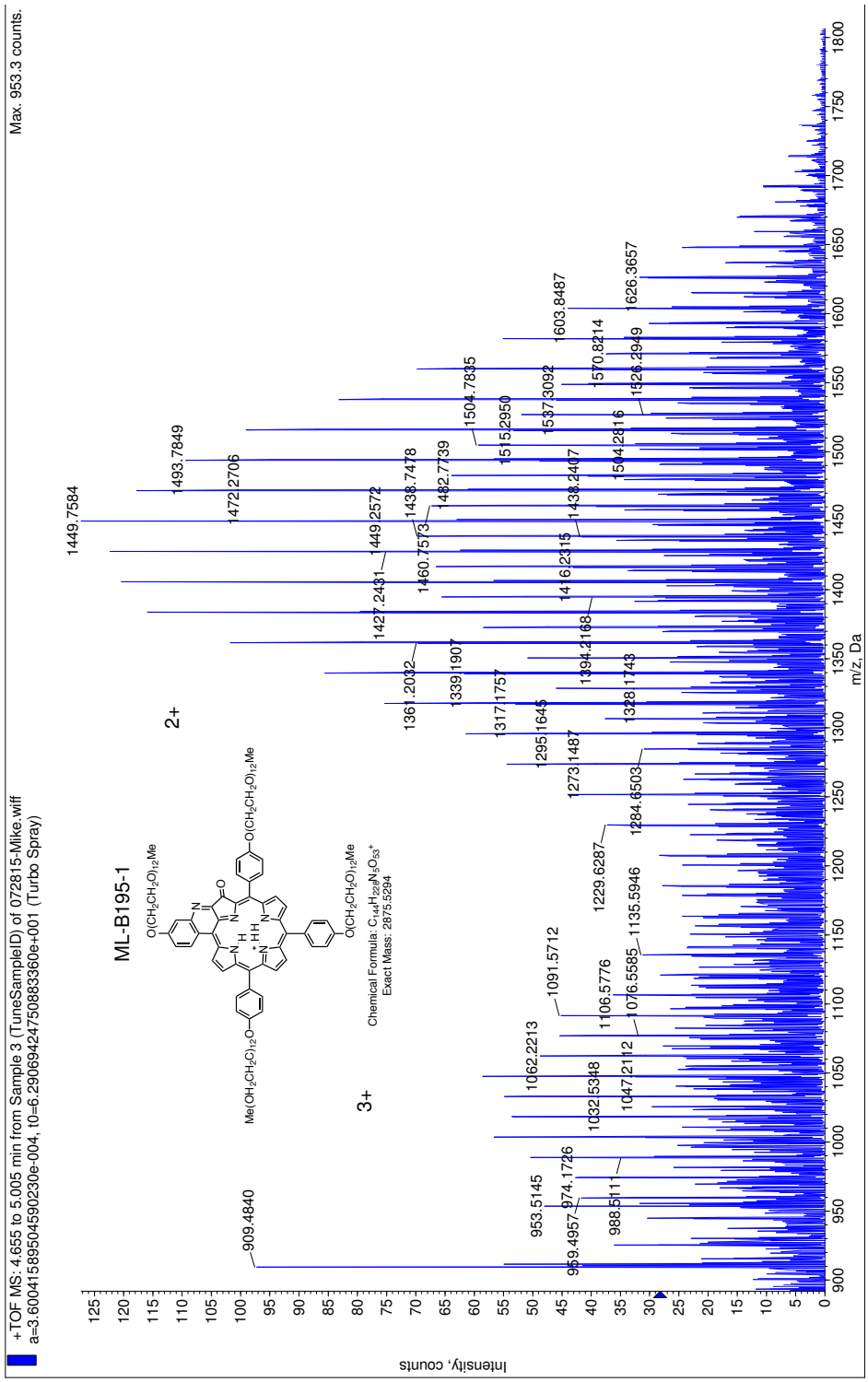

Figure S38. HR-MS (ESI$^+$, 100% CH_3CN, TOF) of **4e**.

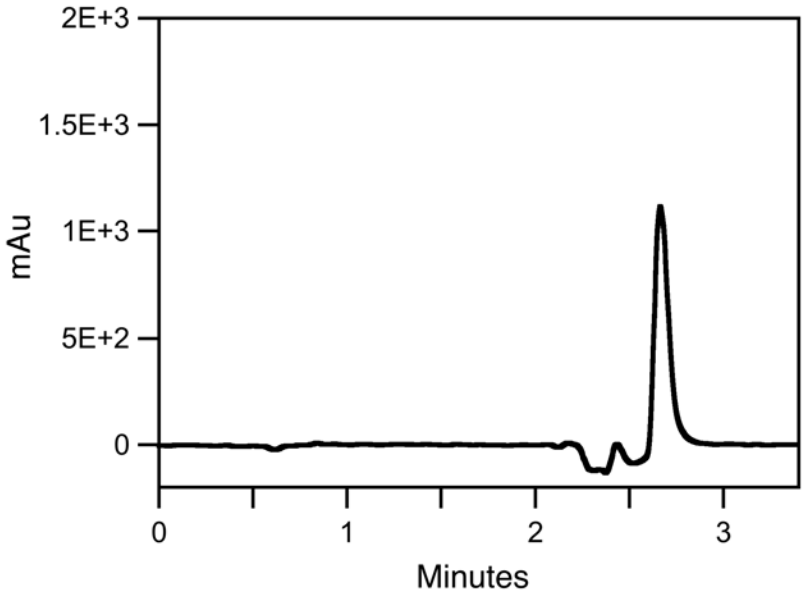

Figure S39. HPLC trace, UV-vis detector, of **4e** (silica, mobile phase: CH_2Cl_2/10% MeOH).

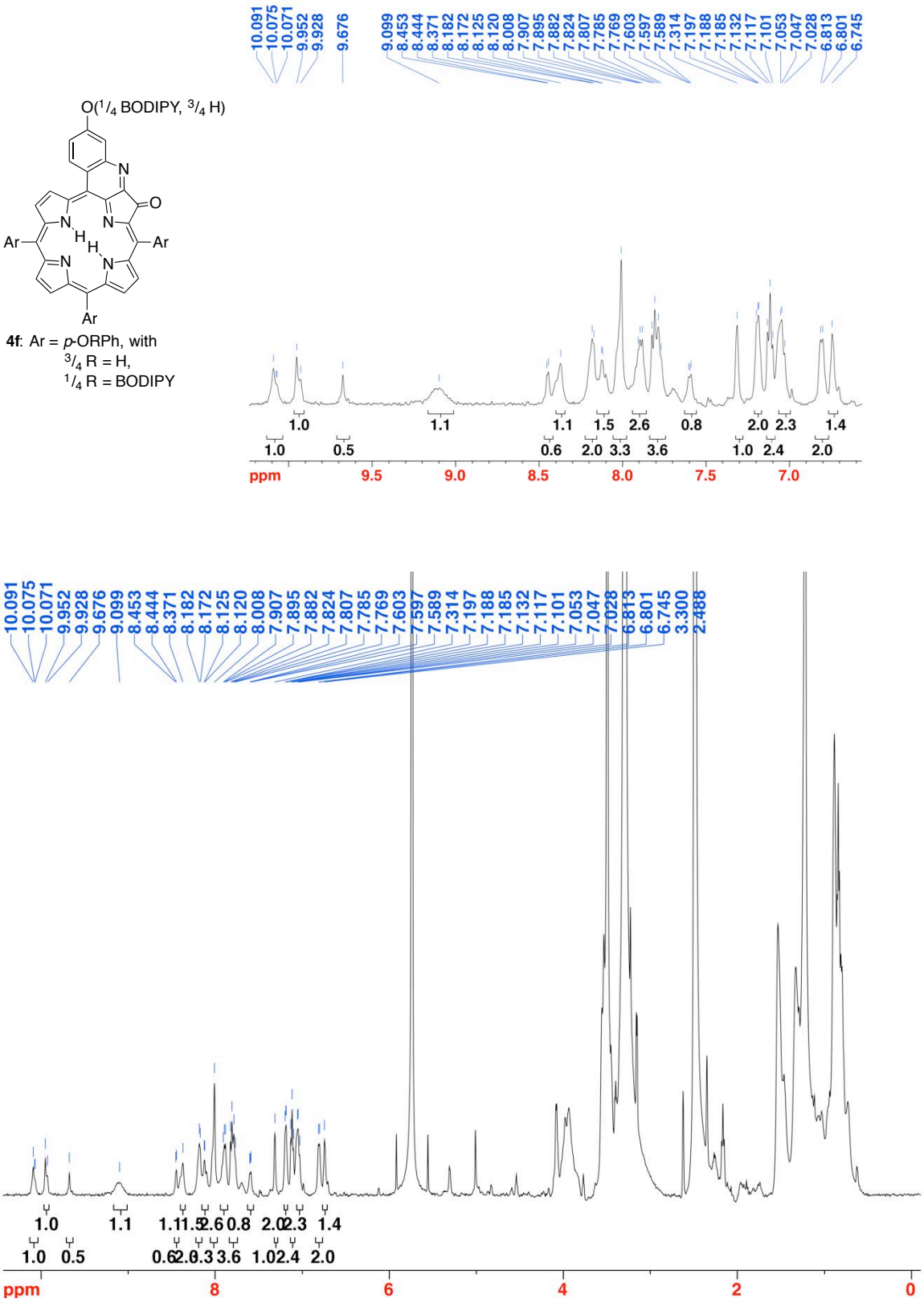

Figure S40. ^{1}H NMR spectrum (500 MHz, DMSO-d_6) of **4f**.

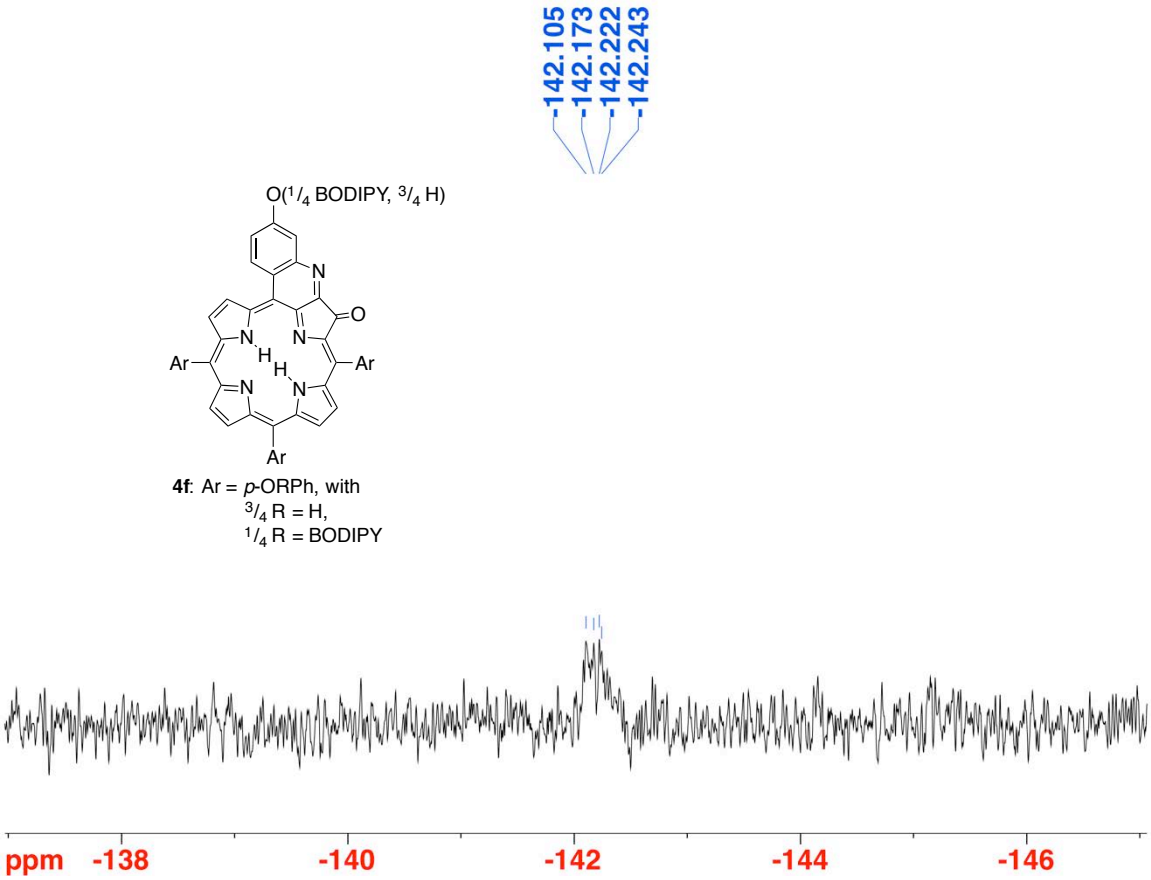

Figure S41. ^{19}F NMR spectrum (470 MHz, DMSO-d_6) of **4f**.

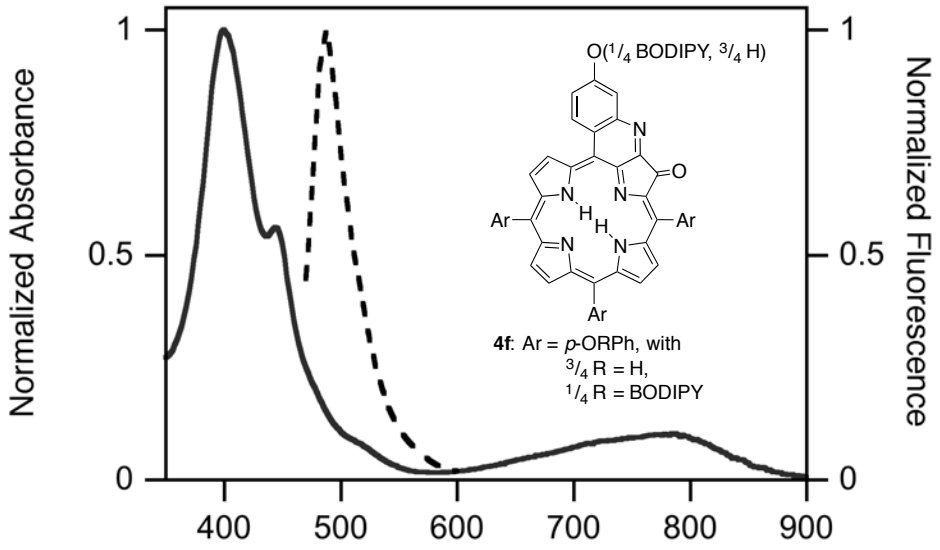

Figure S42. UV-vis and Fluorescence emission spectrum (MeOH, $\lambda_{excitation}$ = 441 nm) of **4f**.

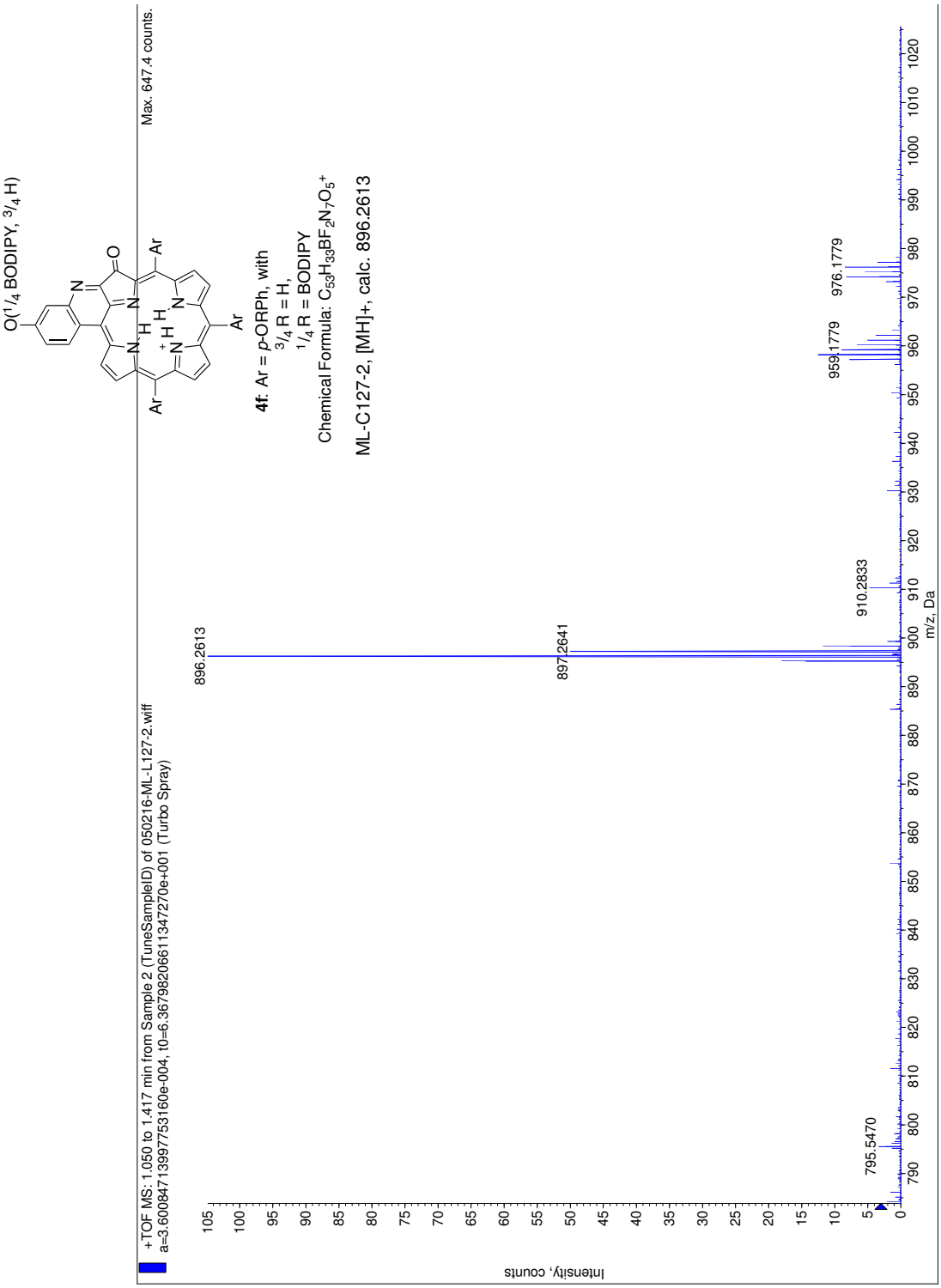

Figure S43. HR-MS (ESI+, 100% CH_3CN, TOF) of **4f**.

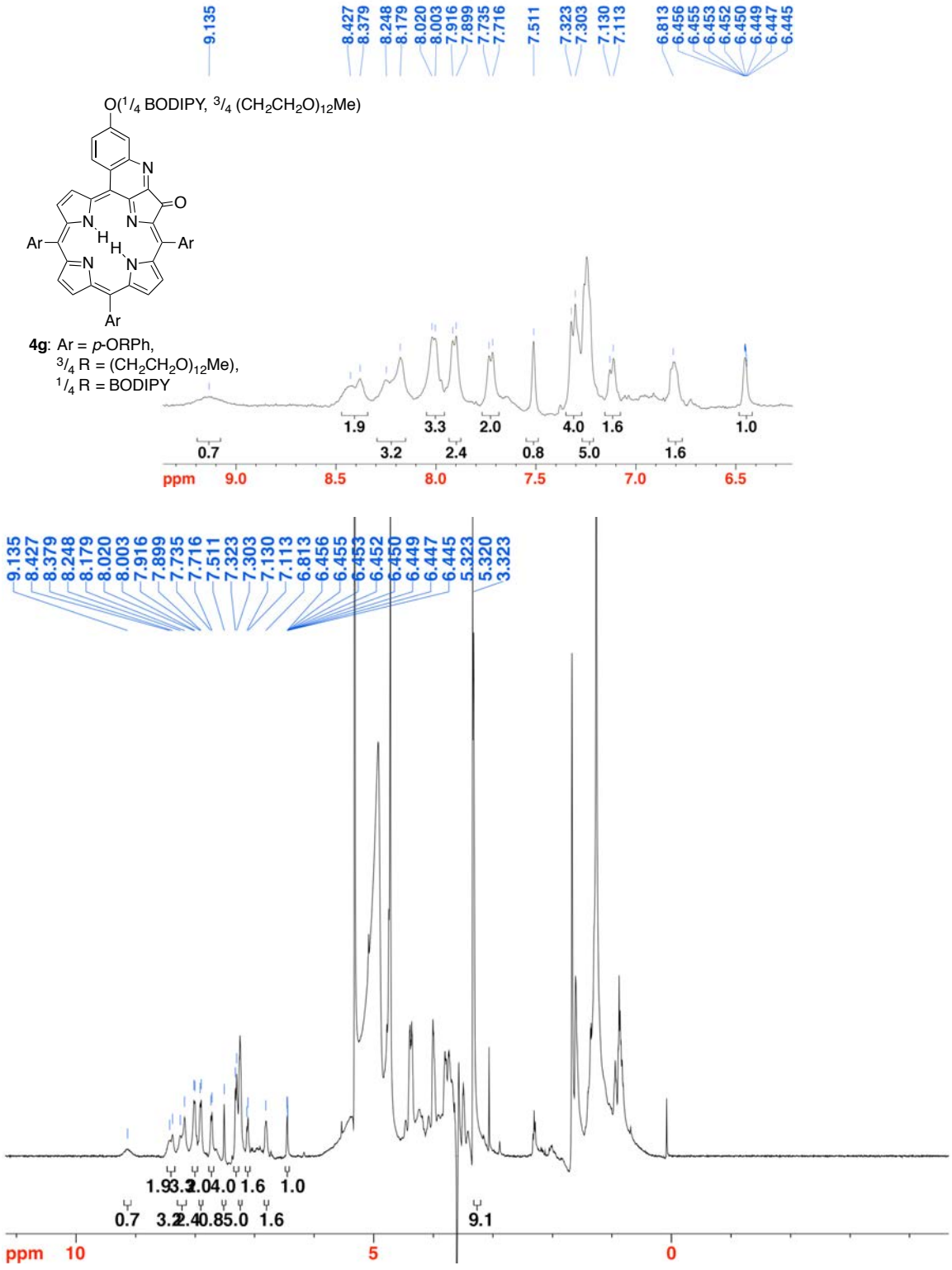

Figure S44. ^{1}H NMR spectrum (400 MHz, CD_2Cl_2, pre-saturated at 3.6 ppm) of **4g**.

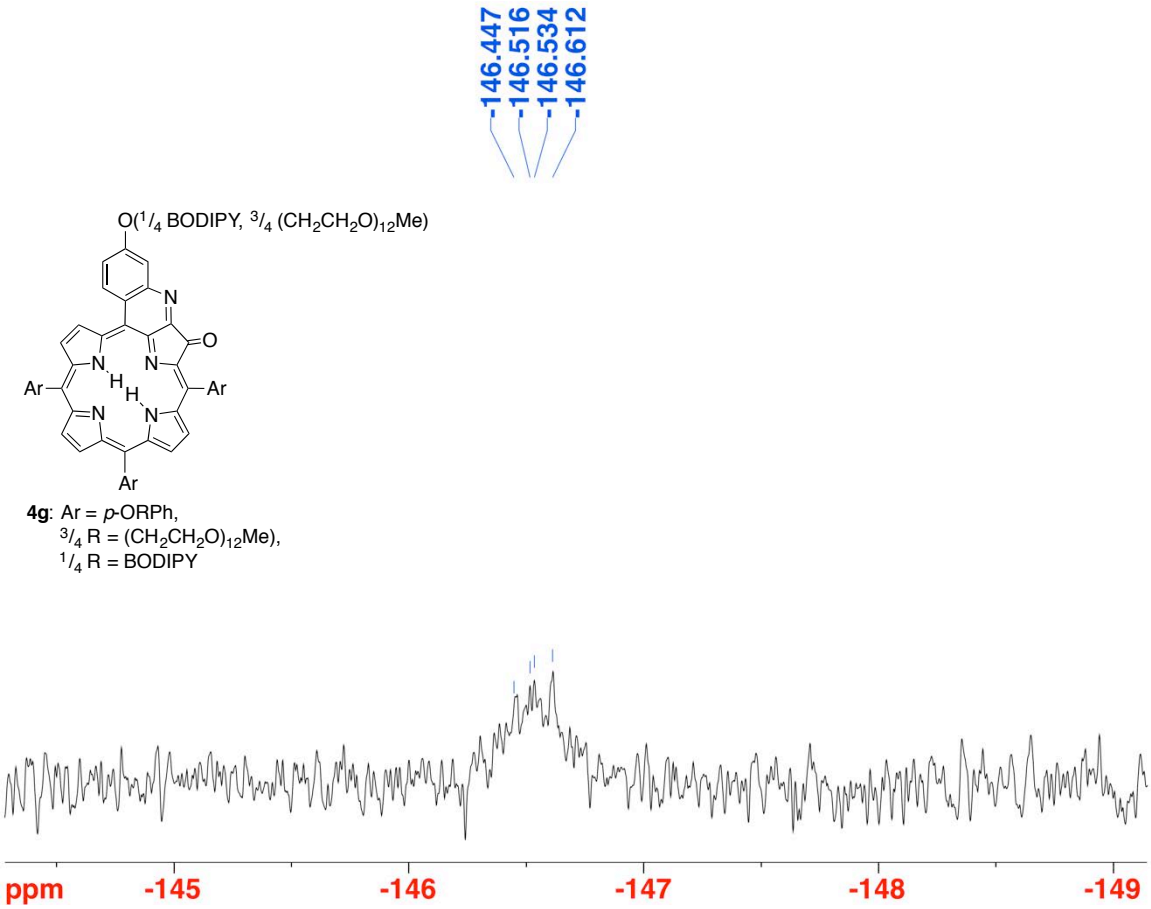

Figure S45. ^{19}F NMR spectrum (376 MHz, CD_2Cl_2) of **4g**.

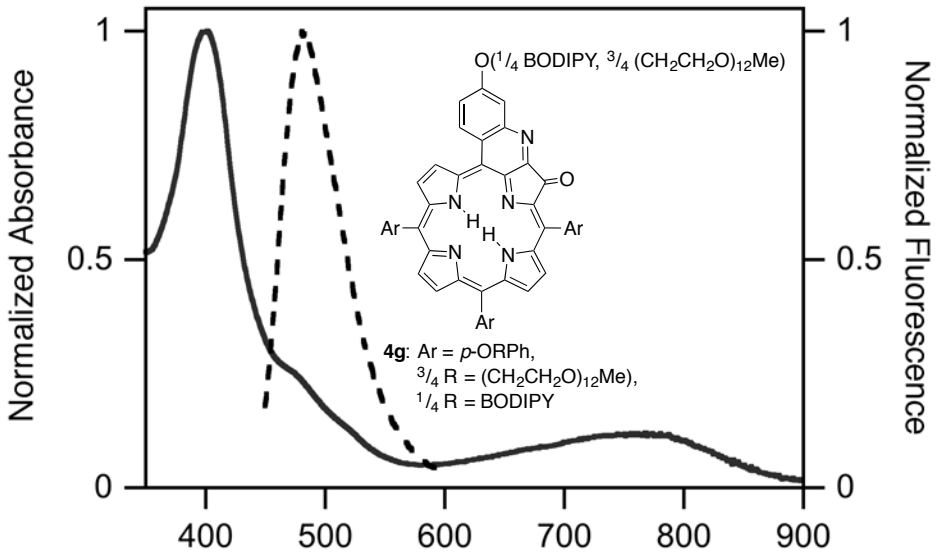

Figure S46. UV-vis and Fluorescence emission spectrum (MeOH, $\lambda_{excitation}$ = 441 nm) of **4g**.

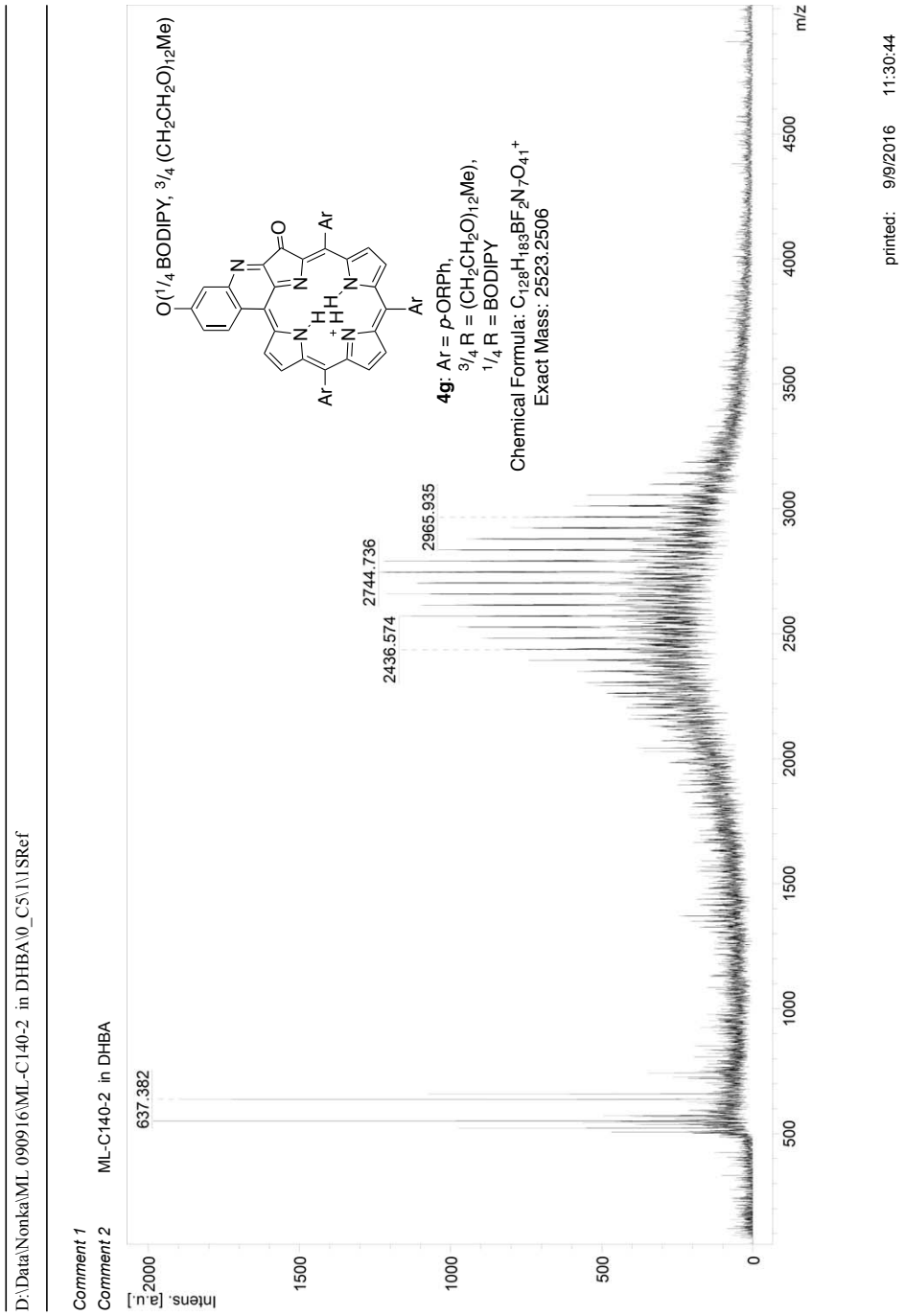

Figure S47. MALDI-TOF spectrum (100% DHBA) of **4g**.

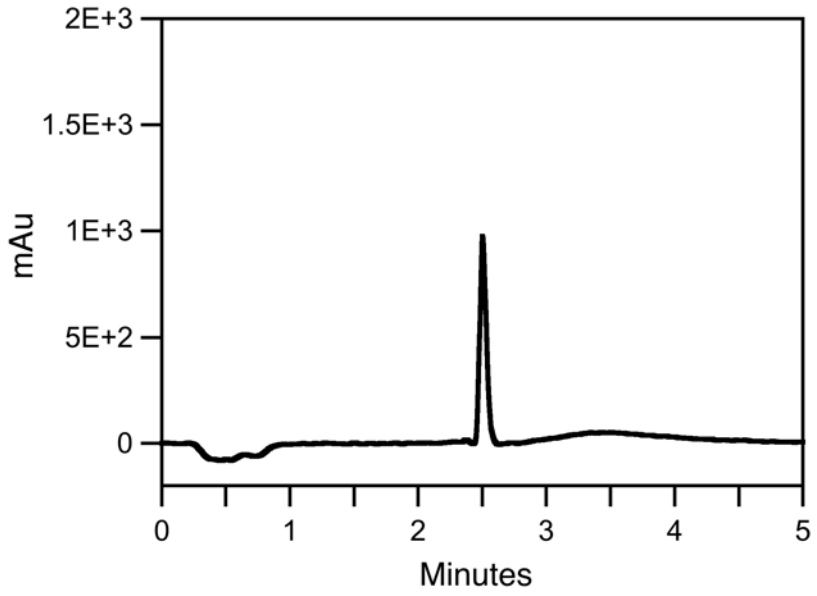

Figure S48. HPLC trace, UV-vis detector, of **4g** (silica, mobile phase: CH_2Cl_2/5% MeOH).

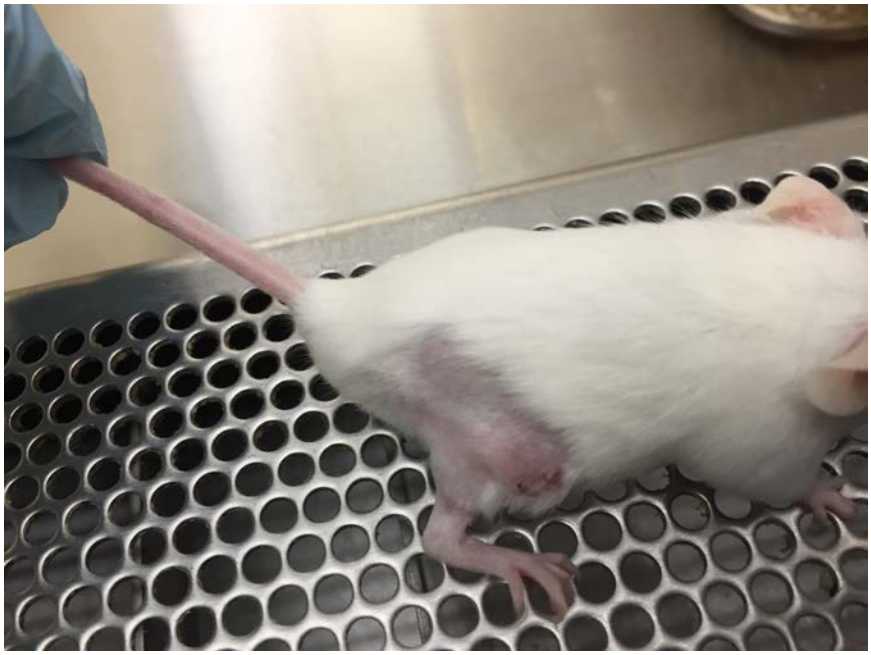

Figure S49. A mouse tumor before injection of **4e**.

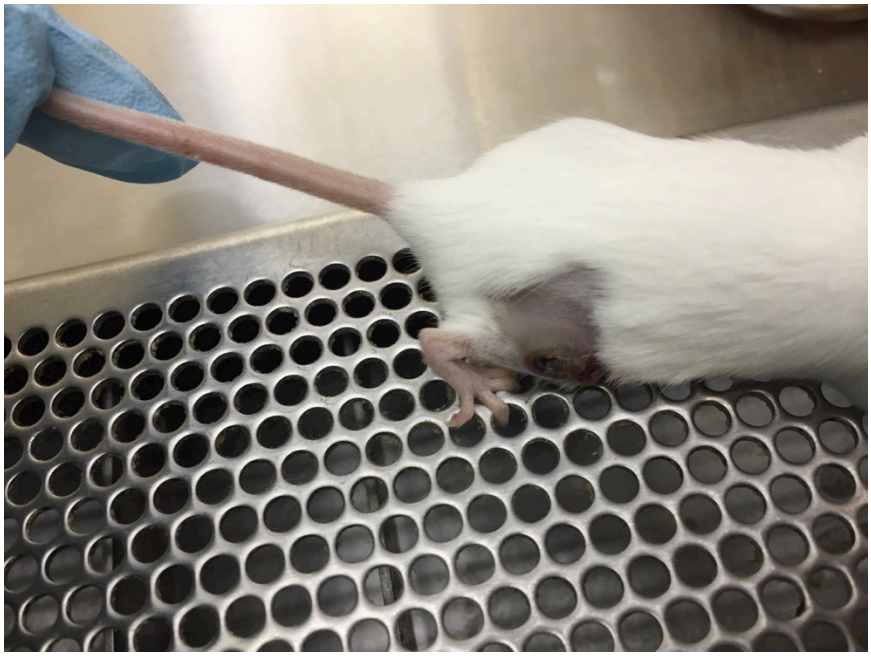

Figure S50. A mouse tumor 48 h after injection of 100 μL of a 33 mM solution of **4e** in PBS, showing the dark brown-stained tumor site.

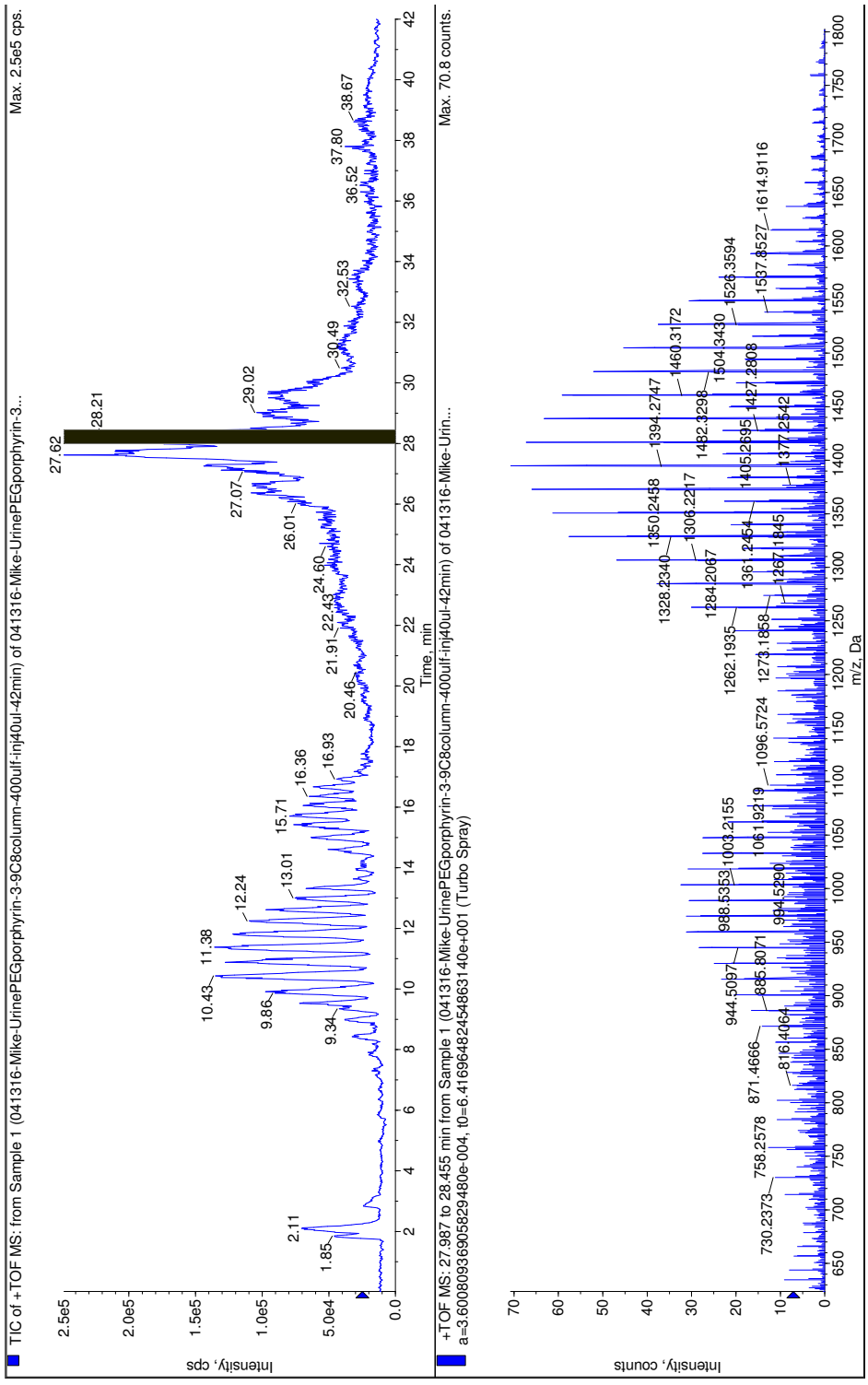

Figure S51. LC-MS of mouse urine extract (CH_2Cl_2), obtained after injection of **4e**.

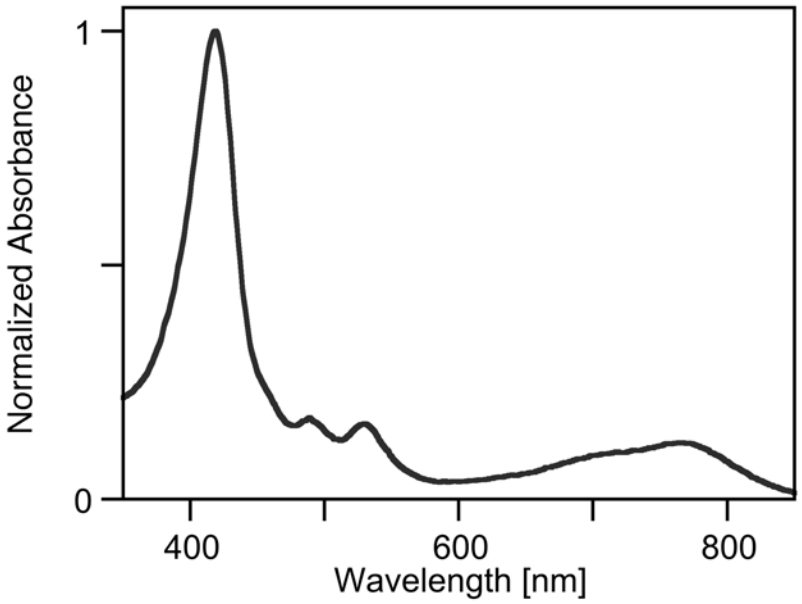

Figure S52. UV-vis spectrum (CH_2Cl_2) of mouse (diluted) urine obtained after injection of **4e**.